

ANALYSIS OF THE DISTRIBUTION OF SPINDLE MICROTUBULES IN THE DIATOM *FRAGILARIA*

DAVID H. TIPPIT, DIETER SCHULZ, and JEREMY D. PICKETT-HEAPS

From the Department of Molecular, Cellular, and Developmental Biology, University of Colorado, Boulder, Colorado 80309. Dr. Schulz' present address is Botanisches Institut der Tierärztlichen Hochschule, Hannover, Bünteweg 17d, D-3000, Hannover, West Germany.

ABSTRACT

The spindle of the colonial diatom *Fragilaria* contains two distinct sets of spindle microtubules (MTs): (a) MTs comprising the central spindle, which is composed of two half-spindles interdigitated to form a region of "overlap;" (b) MTs which radiate laterally from the poles. The central spindles from 28 cells are reconstructed by tracking each MT of the central spindle through consecutive serial sections. Because the colonies of *Fragilaria* are flat ribbons of contiguous cells (clones), it is possible, by using single ribbons of cells, to compare reconstructed spindles at different mitotic stages with minimal intercellular variability. From these reconstructions we have determined: (a) the changes in distribution of MTs along the spindle during mitosis; (b) the change in the total number of MTs during mitosis; (c) the length of each MT (measured by the number of sections each traverses) at different mitotic stages; (d) the frequency of different classes of MTs (i.e., free, continuous, etc.); (e) the spatial arrangement of MTs from opposite poles in the overlap; (f) the approximate number of MTs, separate from the central spindle, which radiate from each spindle pole. From longitudinal sections of the central spindle, the lengths of the whole spindle, half-spindle, and overlap were measured from 80 cells at different mitotic stages. Numerous sources of error may create inaccuracies in these measurements; these problems are discussed.

The central spindle at prophase consists predominantly of continuous MTs (pole to pole). Between late prophase and prometaphase, spindle length increases, and the spindle is transformed into two half-spindles (mainly polar MTs) interdigitated to form the overlap. At late anaphase-telophase, the overlap decreases concurrent with spindle elongation. Our interpretation is that the MTs of the central spindle slide past one another at both late prophase and late anaphase. These changes in MT distribution have the effect of elongating the spindle and are not involved in the poleward movement of the chromosomes. Some aspects of tracking spindle MTs, the interaction of MTs in the overlap, formation of the prophase spindle, and our interpretation of rearrangements of MTs, are discussed.

KEY WORDS mitosis · microtubules · spindle elongation · diatom · clones

Central to understanding the mechanism(s) involved in mitotic movements is an elucidation of the changes in distribution of individual spindle microtubules (MTs) which accompany mitosis. While simple counts of MTs in selected sections along the spindle at different stages of mitosis have been completed for certain cells (2, 4, 5, 8, 9, 14), precise data on the number of spindle MTs, their length, positions of their ends, and the spatial relationships of the various populations of MTs (e. g., "continuous, free, kinetochore, and polar" MTs) have not been forthcoming. Unraveling such structural details in the spindles of most mammalian and higher plant cells is immensely difficult. The much smaller spindles in certain fungi, however, have shown promise in yielding this type of data (6, 7, 16).

The diatom spindle offers unique advantages for such analyses. Its MTs are organized into two distinct groups: (a) those essentially parallel MTs which form a "central spindle" consisting of two half-spindles whose MTs interdigitate in a precise manner to form a central region of overlap; and (b) those MTs which radiate laterally from (or near) the spindle poles into the chromatin and cytoplasm. The central spindle is eminently suitable for precise reconstruction from serial sections. Such reconstructions have already confirmed that during later mitosis, the overlap decreases concurrent with spindle elongation, apparently due to the sliding apart of the half-spindles (12). Pole-

ward movement of chromosomes occurs separately from spindle elongation (separation of the poles) and seems to be associated with lateral MTs and a specific structure, the collar, which encircles each half-spindle. At anaphase, each collar apparently connects the leading edge of the chromosomes to the poles; typical kinetochore MTs have not been identified (18, 20, 24). Thus several mechanisms may be responsible for achieving chromosomal separation (24).

In this paper, the central spindle of *Fragilaria* is reconstructed from transverse serial sections (i. e., by tracking MTs) at all stages of mitosis. From longitudinal sections, the length of the overlap, half-spindles, and whole spindle are measured at different mitotic stages. This colonial diatom is especially suitable for such studies because: (a) The colonies of *Fragilaria* (Figs. 1-3) are flat ribbons of contiguous cells (clones), which remain accurately aligned as they grow and divide. Thus, not only may cells from different ribbons be compared, but more importantly, using a single ribbon of cells (initially identical in size), direct comparisons of spindles at different stages of mitosis can be made with confidence that cellular variability will be minimal. (b) The central spindle contains relatively few MTs; consequently, not only is the accuracy of tracking MTs enhanced, but it involves less work, which permits reconstruction of more spindles for a given amount of effort. (c) Because the spindles are small, it is possible at late anaphase to reconstruct the population of MTs that radiate laterally from the spindle poles (MTs separate from the central spindle).

FIGURE 1 Scanning electron micrograph of a ribbon of cells. Individual cells are contiguous; they adhere side-by-side and remain aligned as they grow and divide. $\times 1,500$.

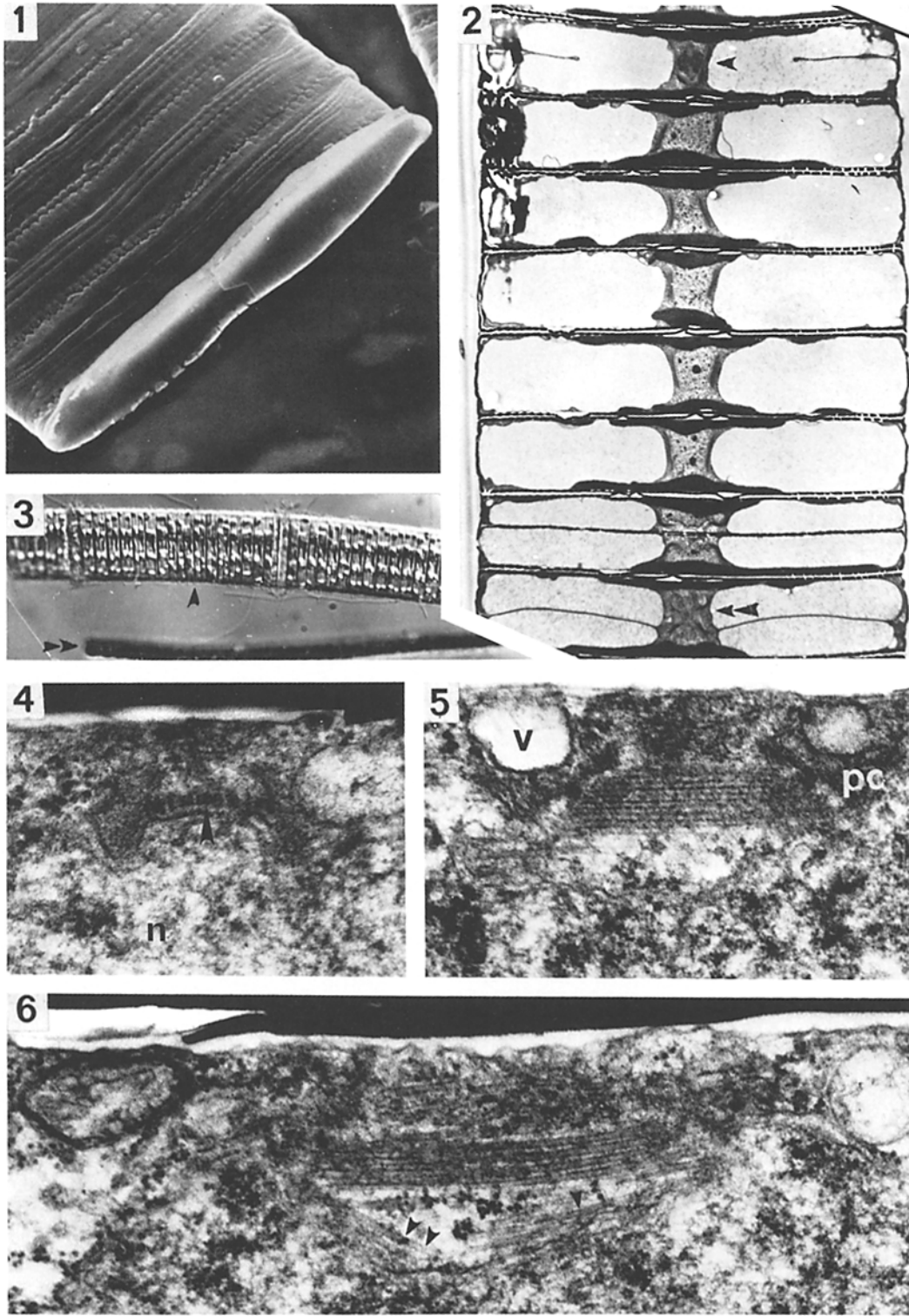
FIGURE 2 A ribbon of cells containing a metaphase (arrow), telophase (double arrow) and recently cleaved cell. $\times 2,100$.

FIGURE 3 Light micrograph of a ribbon of cells (single arrow). The double arrow shows a ribbon viewed from the side.

FIGURE 4 The spindle is initiated outside the nucleus (*n*) when a striated structure (arrow) forms near the MC which is situated above the nucleus. $\times 61,000$.

FIGURE 5 A parallel array of MTs assembles and elongates between the polar complexes (*pc*). A small vacuole (*v*) is invariably associated with each polar complex. $\times 59,000$.

FIGURE 6 The spindle continues to increase in length but numerous MTs (arrows) from the poles now invaginate the surface of the nuclear envelope. Some of these MTs form pockets in the nuclear envelope, which extend into the nucleus, usually parallel to the spindle. $\times 57,000$.



MATERIALS AND METHODS

Fragilaria (identified as *Fragilaria capucina* fo. *mesolepta* Rhb.) was collected from a local stream; cultured material was fixed for electron microscopy as previously described (24).

Terminology

The central spindle is the set of essentially parallel MTs extending between the spindle poles; at metaphase, it consists of two half-spindles which interdigitate at a middle, "overlap" region. The microtubule center (MC), a small dense organelle near the interphase nucleus, is the focus of numerous MTs; it is intimately associated with spindle formation. The polar complex is the structure at each spindle pole. The collar is a ring of amorphous, coherent matrix which encircles certain parts of the central spindle, and to which the chromosomes may attach at anaphase (20, 24).

We use the classification of McIntosh et al. (13) for the different types of spindle MTs: continuous MTs run from pole to pole; free MTs have both ends free in the spindle (i. e., not attached at either pole); polar MTs have one end at the pole and the other end free; kinetochore MTs have one end at the kinetochore. MTs with ends at both a kinetochore and a pole are by definition kinetochore MTs.

Serial Section Analysis

The MTs of the central spindle have been reconstructed from transverse serial sections. The figures (Figs. 23–32) showing the end points of all the central spindle MTs are generated as follows: the serial number of each section in a series through a given spindle, beginning at one pole and extending to the other, is set out along the horizontal axis. Starting at one pole, each MT profile in each section is identified and assigned a position along the vertical axis. When this same MT is positively identified in the adjacent section, its two plotted points are then joined into a line which later is extended to encompass all profiles of this MT along the spindle (see reference 12 for details of MT tracking). MTs present in only one section are displayed as a short bar. Thus a graph is generated which shows in one-dimensional form the end points of each MT and an estimate of their relative lengths. Clearly these figures do not show the spatial arrangement of MTs. The MTs which constitute each half-spindle at prometaphase through telophase are arranged according to length, with the half-spindles set one on top of the other. These diagrams are referred to as reconstructions, although the data are not displayed in three-dimensional form as the term might suggest. To limit cellular variability, several spindles from a single ribbon (as in Figs. 1–3) were reconstructed. Cells at different stages of mitosis rarely lie conveniently side by side within a single ribbon; consequently, we have cut up to 3,200 serial sections per ribbon to obtain one spindle at each stage of mitosis.

Usually a segment of a ribbon containing about 30 cells was sectioned; these represent a clone derived from five divisions.

An estimation of the length of individual MTs was made by counting the number of sections an MT traverses; this technique is subject to error, particularly if the serial sections vary in thickness. Microdensitometric measurements of serial sections, from a single grid, typically indicate a variation in section thickness of up to 8% (14). This variation may increase when two sets of sections, cut and stained separately, are compared. Possible artifactual shrinkage of the cells, cellular variation, and errors in determining the precise ends of the MTs (i. e., occasionally it is not clear if an MT ends in a given section or the next) are other factors which create uncertainty. Although we recognize the likelihood of some errors, certain measurements obtained by this method are still useful, particularly from rows of sections cut in the same day from a single ribbon containing different stages of mitosis (see Results).

Tracking longitudinal MT profiles is done similarly to tracking transversely sectioned MTs; however, such longitudinal tracking is difficult and less accurate.

Measurements of the Spindle from Longitudinal Sections

Each prophase spindle serially sectioned, and the length of the longest MTs extending between the poles, was measured. The spindles were sectioned in two orientations; the spindle in Fig. 7 is sectioned at right angles to the spindle in Fig. 9a. In Fig. 7, the poles are tilted towards each other and the linear distance between the two white arrows indicates the overall length of this particular spindle. The length of the spindle in Fig. 9a is similarly indicated; however, sectioned in this view, the spindle is broader and the poles are more flattened. Here it is necessary to select and do the measurement on the particular serial section which contains the longest MTs. At metaphase, the length of three distinct morphological regions of the central spindle was measured—the overlap, average of the two half-spindles, and the whole spindle. Fig. 13 illustrates where each of these measurements is taken along any spindle. Our measurements of the spindle from longitudinal sections are subjective estimates since the MTs of each half-spindle are not uniform in length; they do not end in the same plane in the overlap or at the pole (Figs. 26 and 29). Our measurements carefully but subjectively attempt to average out such differences; discrepancies between measurements by different persons of the same spindle are $\sim 0.06 \mu\text{m}$ (1.5 mm or more variation in certain spindles, measuring directly on the negatives). Procedural problems such as shrinkage of cells during processing and uneven expansion of sections may also create inaccuracies in the measurements. Although we recognize the possibility of such errors, certain results are significant, particularly when spindles from individual ribbons of cells (clones) are compared.

RESULTS

Brief Description of Mitosis

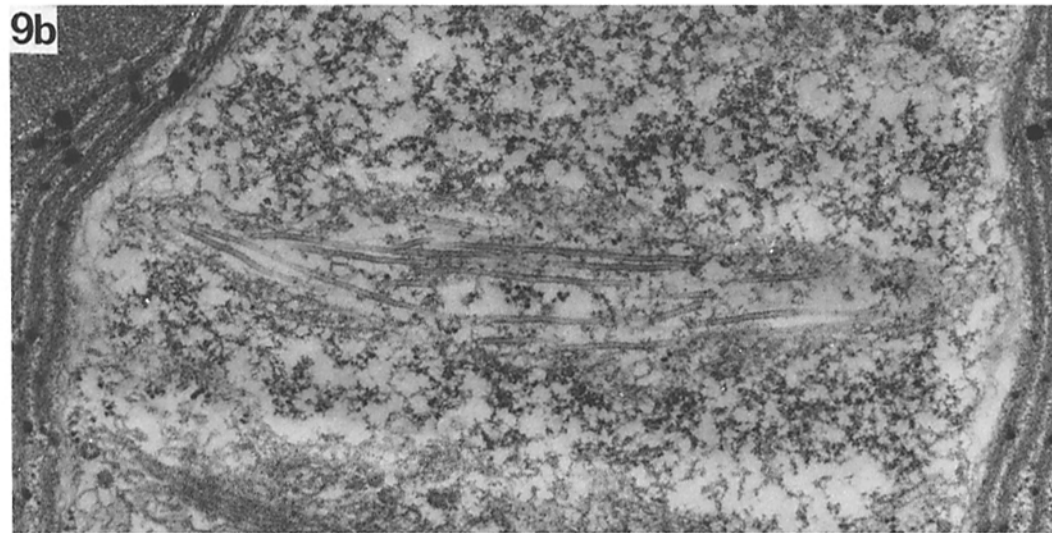
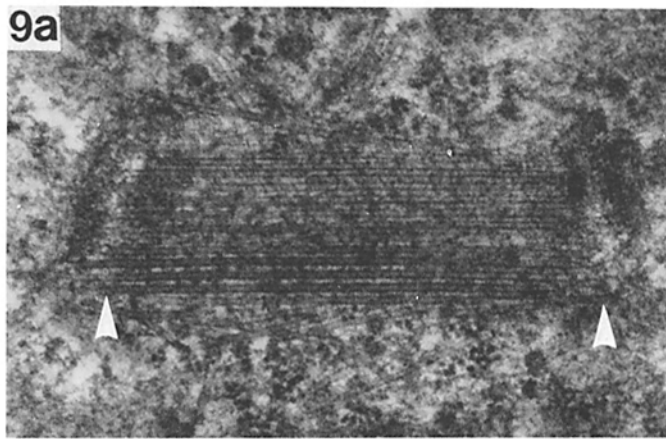
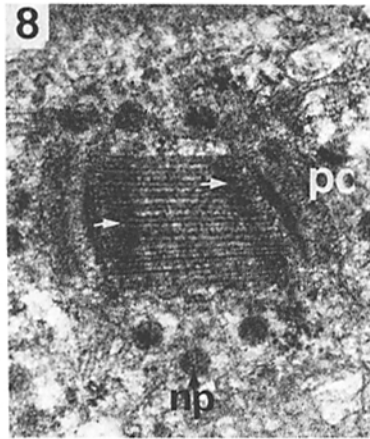
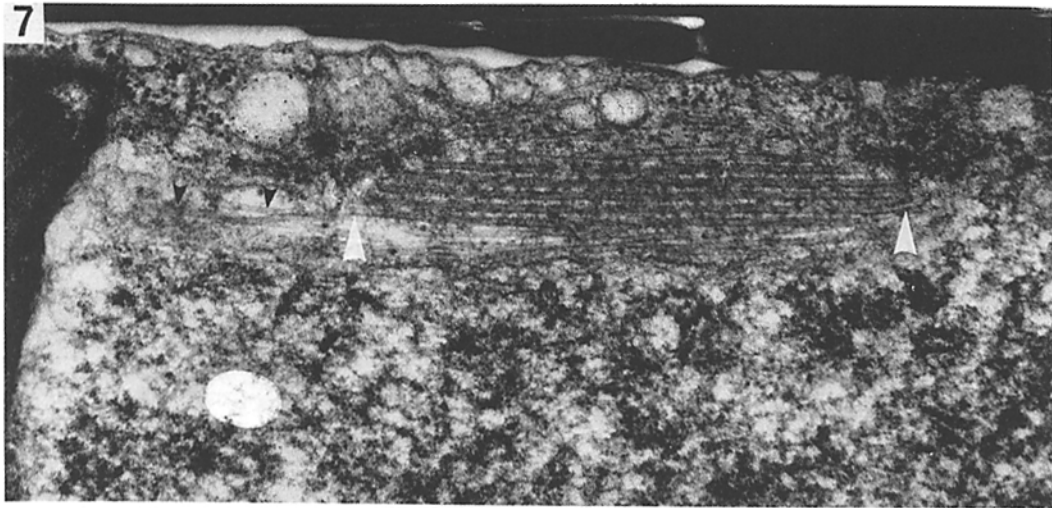
The formation of the spindle in *Fragilaria* is similar to other diatoms (19, 24) and is not described in detail here. The spindle, initiated outside the nucleus at prophase as a striated structure, forms near the MC (Fig. 4, arrow). The ill-defined ends of this structure become the polar complexes and later (Figs. 5–7), a parallel set of MTs assembles and elongates between them. The spindle is a flattened band of MTs; cells sectioned at right angle to these show its broadened aspects (Figs. 8 and 9a). The ends of these MTs are embedded in a dense layer (Fig. 8, arrows). As the prophase spindle elongates, certain MTs begin to invaginate the nuclear envelope (Figs. 6 and 7). Similar MTs are observed in Fig. 9b, which is a section taken from the same spindle shown in Fig. 9a. It is difficult to determine the end points of these MTs; many clearly terminate at one pole and extend past the other pole into an invagination in the nuclear envelope. Transverse sections of prophase spindles are shown in Figs. 10–12. At prometaphase, the nuclear envelope partially breaks down as the spindle enters the nucleus. As in other diatoms, most of the MTs of the central spindle at late prophase apparently run from one pole to the other (Fig. 9a), but by prometaphase, the spindle consists of the two interdigitated half-spindles (Fig. 13). After the spindle enters the nucleus, the chromatin aggregates around the overlap, apparently interacting with the MTs extending laterally from the poles. At metaphase (Fig. 14), the chromatin encircles the central spindle. Numerous MTs which are not part of the central spindle radiate into the chromatin; some appear to end at its leading edge, others pass through the chromatin into the cytoplasm, often overlapping the similar MTs from the other pole. Kinetochores and kinetochore MTs have not been identified. Visible now on each half-spindle is the ring of amorphous material (Figs. 14 and 15), earlier named the collar (24). Each extends from the pole over the surface of the central spindle to, and sometimes touching, the chromatin. Early anaphase spindles were not encountered; this stage undoubtedly passes rapidly. Those MTs, not part of the central spindle and which earlier radiated from the poles, are progressively moved radially back past the poles during anaphase (Fig. 16). The way the chromosomes attach to the spindle is not clear. Each mass of chromatin partially en-

velops its collar by late anaphase. The collar also either moves polewards or else is transported polewards by the moving chromatin (Fig. 16, arrows). The arrangement of MTs in the central spindle is altered during anaphase; unlike metaphase, they are now distinctly bowed outwards near the poles (Fig. 16, small arrows), while the overlap remains tightly constricted. The chromatin moves past the polar complex (Fig. 16); this is also observed in Fig. 17 (a cell sectioned at right angles to that in Fig. 16), but some chromatin on one side remains at the pole, perhaps obstructed by the chloroplast. Transverse sections of metaphase and telophase spindles are shown in Figs. 18–22. Later, the polar complexes separate slightly from the central spindle. The ingrowing edge of the cleavage furrow soon bisects the spindle, whose remnants disappear. Each polar complex remains outside the reforming nuclear envelope. Later, a new MC arises near or directly from the polar complex. The new MC then moves around its daughter nucleus to the surface of the cleavage furrow to where the silicalemma is initiated.

Analysis of the Spindle from Transverse Sections

The central spindles of 28 cells (12 prophases, 1 prometaphase, 6 metaphases, 7 anaphases, and 2 telophases) have been reconstructed from serial sections. Because many of these spindle reconstructions for a given stage of mitosis are very similar, only 10 representative reconstructions are presented in this paper (Figs. 23–32). Above each reconstruction is a distribution profile derived from the total number of MTs in each section along the same spindle. The position of chromatin in each spindle is indicated on the reconstruction by cross-hatching on the bottom of the diagram. A comparison of these reconstructions at different stages of mitosis reveals the changes in the distribution of MTs in the central spindle. The validity of inferences derived from such cell-to-cell comparisons are naturally affected by procedural problems and cellular variability. To limit the latter, entire ribbons of cells (clones) were serially sectioned. Thus, of the 28 reconstructions, seven are from one such ribbon, six and five are from two others. The remaining 10 reconstructions are usually derived from a single cell from other ribbons.

CHANGES IN THE DISTRIBUTION OF MTS
IN THE CENTRAL SPINDLE DURING MITO-



sis: Longitudinal sections indicate that most of the prophase spindle MTs extend from pole to pole. The reconstructed spindles show variation in MT length, especially during later prophase (Figs. 26 and 27). Most of this length variation results from the polar complexes being tilted towards one another (Fig. 7). For example, in Fig. 26, all but seven MTs in this spindle are continuous because one polar complex can be traced through sections 5–8 and the other through 12–14 (see section entitled, Frequency of . . . , for further discussion). Comparison of different prophase spindles shows that these continuous MTs increase in length (Figs. 23–27) and number (see section entitled, Total number . . .). Between late prophase and prometaphase, the spindle is transformed into two interdigitated half-spindles devoid of continuous MTs and comprised mainly of polar MTs (compare Figs. 27 and 28). This transition is rapid, because intermediates undergoing this important change have not been encountered in the nearly 85 prophase and metaphase cells examined. By metaphase (Fig. 29), the ends of the MTs from each half-spindle in the overlap are not coplanar, because their MTs have slightly different lengths. At prometaphase, metaphase, and early anaphase, the peak in the MT distribution curves (Figs. 28–30) correspond in position to the overlap. During late anaphase (Fig. 31) this peak declines, to be replaced by a central dip at telophase (Fig. 32). The few MTs remaining in the overlap are the longest in each half-spindle; thus the overlap is reduced to their ends (Fig. 21).

TOTAL NUMBER OF MTS CONSTITUTING THE CENTRAL SPINDLE DURING MITOSIS: Table I shows the total number of MTs (i.e., both

half-spindles) in the central spindles of 30 cells at different stages of mitosis (included are two cells incompletely tracked due to the loss of one to three sections). The prophase spindles are divided into three stages according to their length (as measured in sections); the early prophase spindles were either two or three sections long, the mid prophase are four to seven sections long, and late prophase are eight sections or longer. As the prophase spindle elongates, its MTs proliferate (Figs. 10–12), to a maximum of 86 in one spindle (Fig. 12). When prophase spindles from the same ribbon of cells are compared, the longer spindles (as measured in sections) invariably contain a larger number of MTs. At metaphase, the central spindle contains between 46 and 50 MTs (depending upon the cell selected); at anaphase it contains 41–50; at telophase it contains 38–46. Within a single ribbon of cells (clones) which contain at least three spindles at either metaphase, anaphase, or telophase, the number of MTs in the central spindle is 44 ± 6 in one ribbon (the cells shown in Figs. 29, 30, and 32), 47 ± 1 , and 45 ± 2 , in two others. Accordingly, the number of MTs constituting the half-spindles varies; the minimum observed was 19, the maximum 26. Within any given cell, the two half-spindles often, but not always, contain identical numbers of MTs; the maximum variation observed between them was two (in a single spindle, one half-spindle had 23 MTs and the other 21).

These data show that the number of central spindle MTs rises during prophase to a peak value of about 40% more than the number of MTs in the central spindle after metaphase (see Discussion).

FIGURE 7 The spindle further elongates, and most of its MTs still appear to extend from pole to pole. Some MTs (small dark arrows) extend past the polar complex and into the nucleus. The length of 51 prophase spindles was measured (see text). The spindle length is the linear distance between the longest MTs (i.e., between the two white arrows- $1.36 \mu\text{m}$); other prophase spindles were similarly measured. See Fig. 9a. $\times 53,500$.

FIGURE 8 The forming prophase spindle sectioned at right angle to the cells in Figs. 4–7. The spindle is broader in this view and is situated in a small indentation in the nucleus; numerous nuclear pores (*np*) are visible. The MTs near each polar complex (*pc*) are embedded in a dense material (arrows). $\times 35,000$.

FIGURE 9(a and b) As in Fig. 8, except a later stage of prophase. These two micrographs are from a series of serial sections. As sections proceed through the elongated spindle (Fig. 9a) into the nucleus (Fig. 9b), MTs extend across the nucleus again indenting the nuclear envelope. Many of these clearly extend past the polar complexes (which are out of the plane of the section). Such MTs are probably equivalent to those seen in Fig. 7, small arrows. The prophase spindle length in this view (Fig. 9a) is defined as the linear distance between the arrows ($1.27 \mu\text{m}$). 9a = $\times 51,500$. 9b = $\times 38,000$.

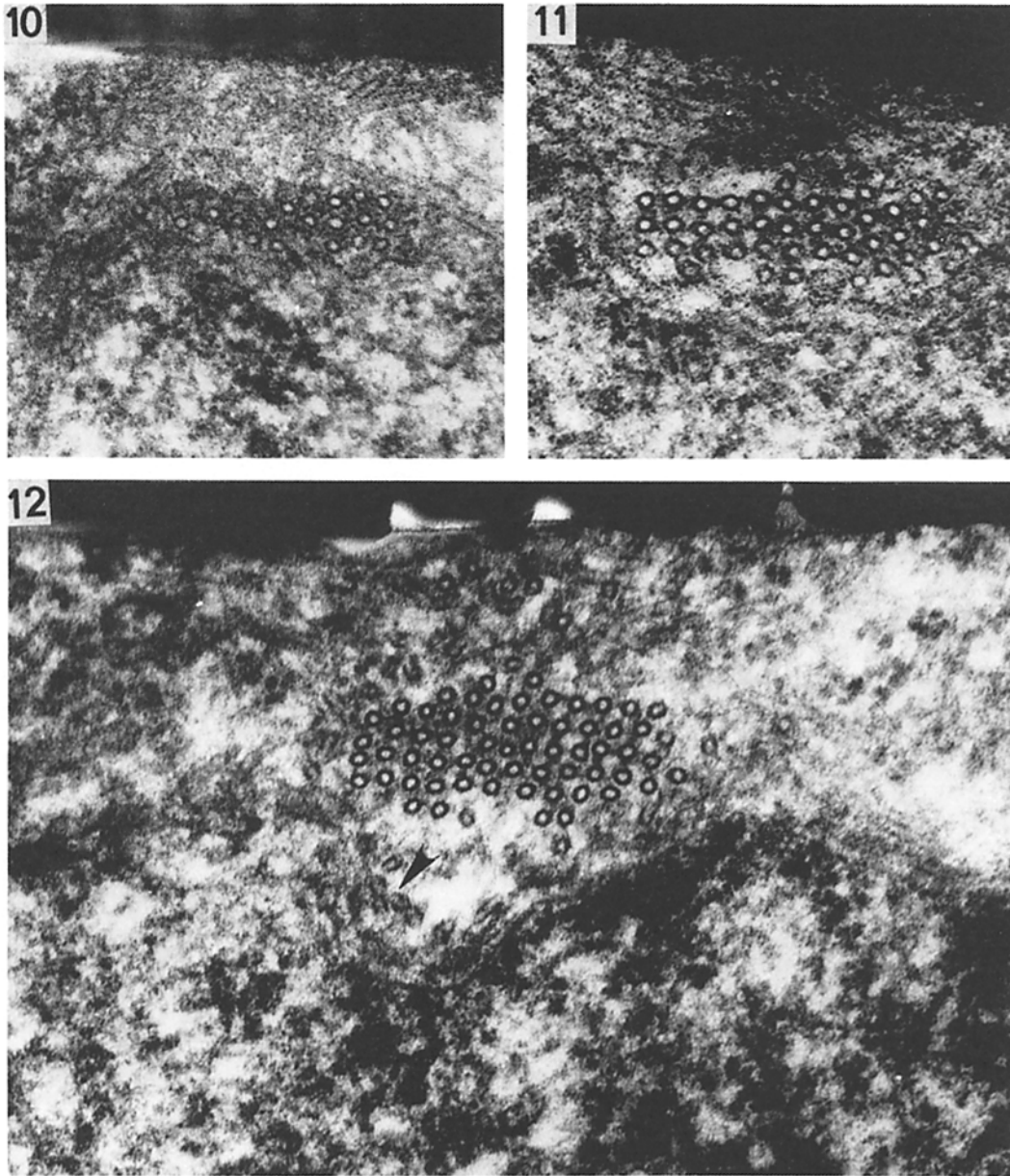


FIGURE 10 Early prophase spindle sectioned transversely. This micrograph is from the spindle reconstructed in Fig. 23. This spindle is two sections long and in this section contains only 18 MTs. $\times 58,500$.

FIGURE 11 Mid-prophase sectioned transversely. The number of MTs increases. The MTs display areas of square close packing. This micrograph is from the spindle reconstructed in Fig. 24. $\times 80,000$.

FIGURE 12 Late prophase sectioned transversely. The number of MTs further increases. This section contains 76 MTs including those marked with the arrow, which can be tracked using an electron microscope equipped with a goniometer stage. This micrograph is from the spindle reconstructed in Fig. 27; there are 86 MTs in this spindle. $\times 91,000$.

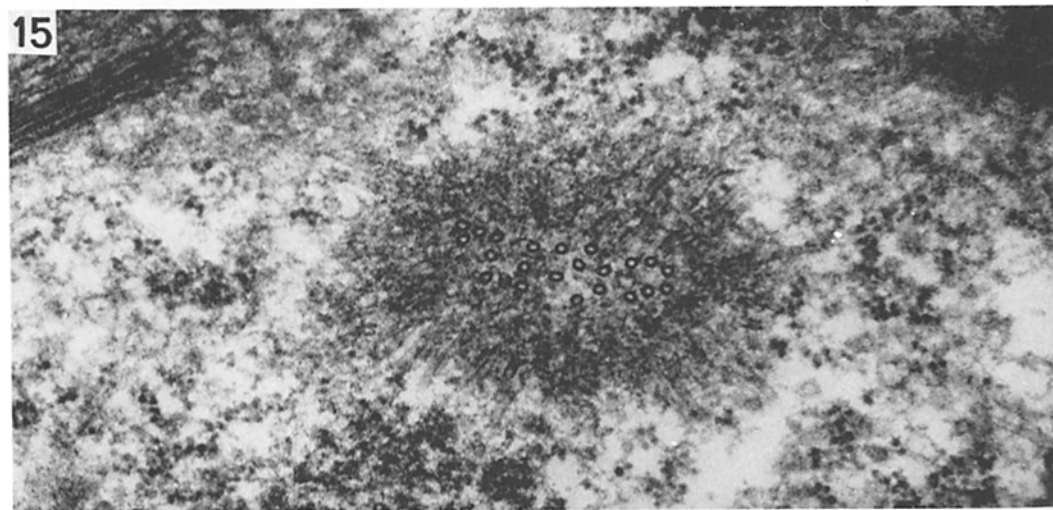
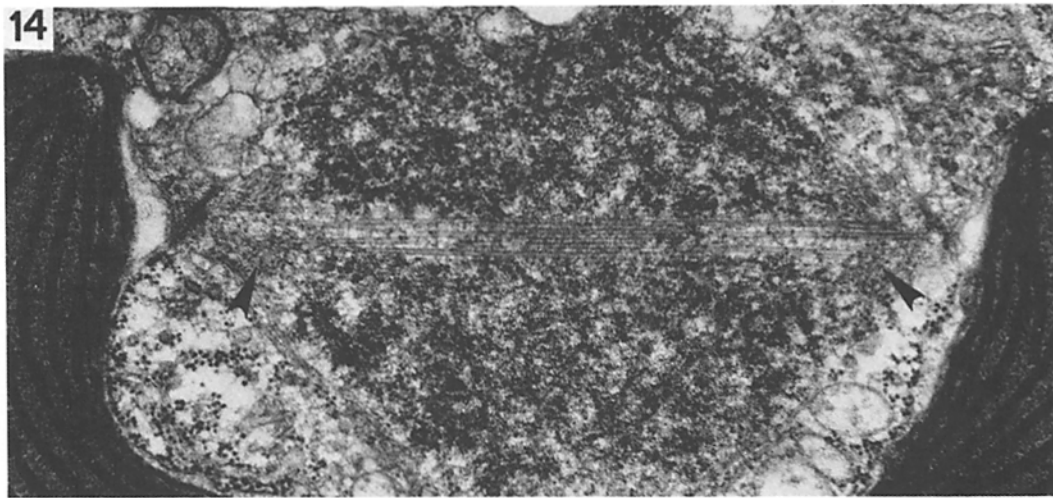
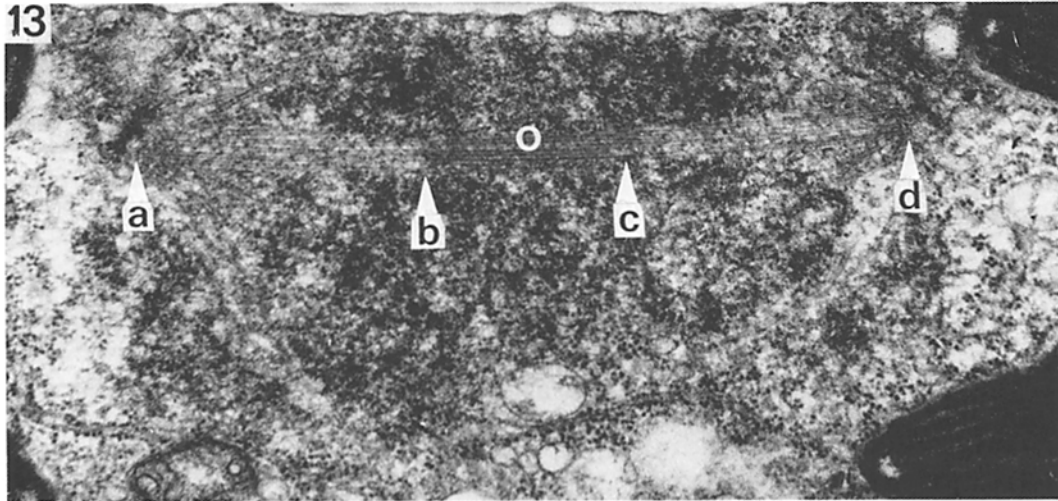
INDIRECT LENGTH MEASUREMENTS OF INDIVIDUAL MTS CONSTITUTING THE CENTRAL SPINDLE: We have determined the length of individual MTs in these spindles by counting the number of sections each MT traverses. Fig. 33 shows the length of each MT of the central spindle from the metaphase, anaphase, and telophase spindles shown in Figs. 29, 30, and 32; these cells are clones. By plotting the MT lengths (see caption to Fig. 33), a curve is generated from each central spindle. The three curves thus created for the metaphase, anaphase, and telophase cell are remarkably similar. If some of their MTs had significantly changed in length during mitosis, the curves could not have coincided in this fashion. In a second ribbon containing three stages of mitosis, the telophase spindle was more irregular, with several slightly shorter MTs. When such curves (i.e., Fig. 33) are derived instead from spindles from different ribbons, more variation is encountered. Never could this variation be related to the stage reached in mitosis; the variation between metaphase spindles is as great as that between metaphase and telophase spindles.

The data on the lengths of individual MTs can also be used to estimate the size of the overlap and the whole spindle. In three mitotic cells from the same ribbon, the metaphase spindle (Fig. 29) contains 46 MTs; 22 MTs from one half-spindle overlap with the 22 MTs from the other half-spindle and the maximum extent of overlap (sections 11–20) is 10 sections (the average length of overlap is only 7.9 sections). In the anaphase spindle (Fig. 30), the 23 MTs in one half-spindle interdigitate with 25 from the other and the maximum extent of overlap is 10 sections. By telophase (Fig. 32), of the 19 MTs in each half-spindle, seven from one half-spindle remain interdigitated with eight from the other, and the extent of overlap is only three sections (sections 17–19). The total spindle length of these three cells is about 27, 29, and 34 sections respectively. These numbers are obtained by averaging the end points of all the individual MTs that terminate at the pole, then measuring spindle length. Similar results were obtained from a second ribbon. The decrease in overlap from metaphase to telophase accompanies two morphological changes in the distribution of MTs. First, the number of MTs in the overlap decreases (Figs. 28–32, distribution curves). Secondly, a few MTs at telophase still

overlap with some from the opposite pole, but the length of this overlapping region is smaller than at metaphase.

FREQUENCY OF DIFFERENT TYPES OF MTS IN THE CENTRAL SPINDLE: The percentage of polar, free, and continuous MTs in the central spindle is given in Table II; kinetochore MTs have not been identified (and possibly do not exist in some diatoms [18, 20, 24]). At prophase (Figs. 23–27), the spindle contains predominantly continuous MTs; careful inspection confirms that most shorter MTs run from pole to pole, their shorter length apparently resulting from the polar complexes being tilted toward one another. Even at metaphase when each polar complex is flat, all the MTs do not end in the same section (i.e., Fig. 29—the MTs from one pole end in sections 1 and 2 and those from the other pole in 27 and 29). Therefore, we would expect the prophase MTs to display even more variation in length since the poles are tilted. 91% of the prophase spindle MTs have been confirmed as continuous. The remaining 9% could not be definitely thus identified; these MTs usually end within one section of the pole and thus it is a subjective judgment as to whether they actually touch the pole or not. Of this 9%, we expect some to be free, others to be continuous and polar. Not included in the numbers of prophase MTs are those which extend behind the poles, away from the spindle (see Fig. 26; in Fig. 27 the nine MTs at the top of the reconstruction extend behind the pole); only the MTs between the poles are included in Table II. After prophase, the central spindle contains predominantly polar MTs. Only one of the 16 spindles examined after prophase contained continuous MTs; this particular spindle contained a single continuous MT (see Discussion). Free MTs are present in small numbers, although some spindles are devoid of them.

TRACKING MTS WHICH ARE NOT PART OF THE CENTRAL SPINDLE: Separate from the central spindle is a group of MTs which extend laterally from each pole. At metaphase (Fig. 14), these run past the collar towards the chromatin. At late anaphase and telophase, they become nearly perpendicular to the central spindle (Fig. 22). Because these MTs are essentially longitudinal during later mitosis, they can be tracked through serial sections. Fig. 34 is such a reconstruction from six serial sections. In four different spindles, the number of these MTs at each pole



greater than $\sim 0.6 \mu\text{m}$ in length is 29 ± 5 .

SPATIAL ARRANGEMENT OF MTS IN THE CENTRAL SPINDLE: The MTs of all the early- and mid-prophase spindles display regions of square packing (Figs. 10–11). The MTs of the late prophase spindle contain some small areas of square- and others of hexagonal-packed MTs (Fig. 12); the majority of MTs have an arrangement in between square- and hexagonal-packing (see Discussion, Figs. 36 and 37). Figs. 35*a–f* are tracings of MTs from six consecutive serial sections of the metaphase central spindle reconstructed in Fig. 29; this series starts in the overlap at section 15 (Fig. 29) and proceeds through the section 20, which cuts through one half-spindle. The filled circles denote the MTs from one pole, while the empty circles show those from the other. Two important facts emerge about the overlap (Fig. 35*a*): (*a*) MTs from one pole tend to be surrounded by those from the other pole, and (*b*) the MTs show a tendency toward square packing on the left, and hexagonal packing on the right, with a more variable region in between. The preferential packing of MTs from opposite poles in the overlap shown in Fig. 35*a* is characteristic of all 16 spindles examined after metaphase. (A statistical analysis of MT packing in *Diatoma* is in preparation by McDonald, Edwards, and McIntosh.)

As the sections move from the overlap towards one pole (Figs. 35*b–f*), MTs from one half-spindle drop out until those remaining after Fig. 35*f* belong solely to the other half-spindle. The arrangement of MTs in the overlap therefore influences their arrangement just outside the overlap, and at metaphase this arrangement also remains fairly constant along the length of the half-spindle (compare Figs. 18 and 19). In contrast, by anaphase and telophase, the MTs nearer the pole have usually aggregated, sometimes into two groups (Fig. 20).

Measurements of the Spindle from Longitudinal Sections

Measurements were made from 51 prophase, 14 metaphase, 5 anaphase, and 9 telophase spindles. The length of the shortest prophase spindle observed is $0.18 \mu\text{m}$; the longest is $1.36 \mu\text{m}$. The lengths of the remaining 49 prophase spindles measured are evenly distributed within this range. The data indicate that the prophase spindle increases in length up to at least $1.36 \mu\text{m}$. Between prophase and prometaphase, the central spindle is transformed into two interdigitated half-spindles (compare Figs. 9*a* and 13 with Figs. 27 and 28). Accompanying this change is an increase in total spindle length; the longest prophase spindle recorded was $1.36 \mu\text{m}$, while the shortest prometaphase is $2.41 \mu\text{m}$. We have sectioned nearly 85 prophase and metaphase cells (some were not used for technical reasons) for this paper and have not encountered intermediates in spindle length. Between prometaphase and telophase, the length of three distinct morphological regions of the central spindle are measured—the overlap, average of the two half-spindles, and the whole spindle. Different cells at the same stage of mitosis exhibit considerable variation in spindle length and half-spindle length (Table III); consequently, it is not possible to accurately assess changes in their length. The overlap at telophase is consistently smaller than at metaphase. Table IV shows two groups of metaphase, anaphase, and telophase spindles which are clones. Here, the overlap decreases from metaphase to telophase, while the spindle length increases; the length of the half-spindles does not vary significantly.

DISCUSSION

Various characteristics of the diatom spindle make it useful for studying the mechanism(s) of mitosis,

FIGURE 13 Prometaphase. The spindle now consists of two interdigitated half spindles. Numerous MTs not part of the central spindle radiate from the poles towards the chromatin, which begins to aggregate around the overlap (*o*) of the central spindle. The length of the half-spindles, whole spindle, and overlap was measured (see Results). These parameters of the spindle are as follows: overlap length is the linear distance between *B* and *C* ($\sim 0.69 \mu\text{m}$); whole-spindle length is the linear distance between *A* and *D* ($2.62 \mu\text{m}$); the half-spindles are the distances between *A* and *C* ($1.64 \mu\text{m}$) for one half-spindle, and between *B* and *D* ($1.64 \mu\text{m}$) for the other. $\times 39,000$.

FIGURE 14 Metaphase. The chromatin encircles the central spindle. Two regions of amorphous material named “collars” (arrows) encircle the central spindle near each pole. $\times 34,500$.

FIGURE 15 A micrograph of a section through the “collar,” which is the ring of amorphous material which surrounds the central spindle near each pole. $\times 65,000$.

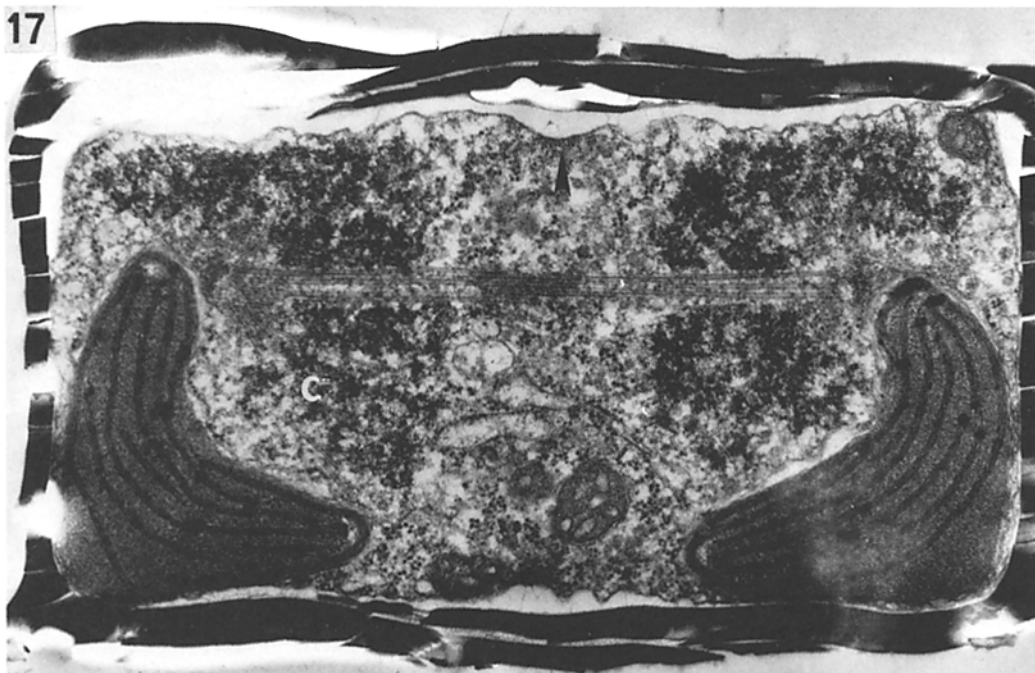
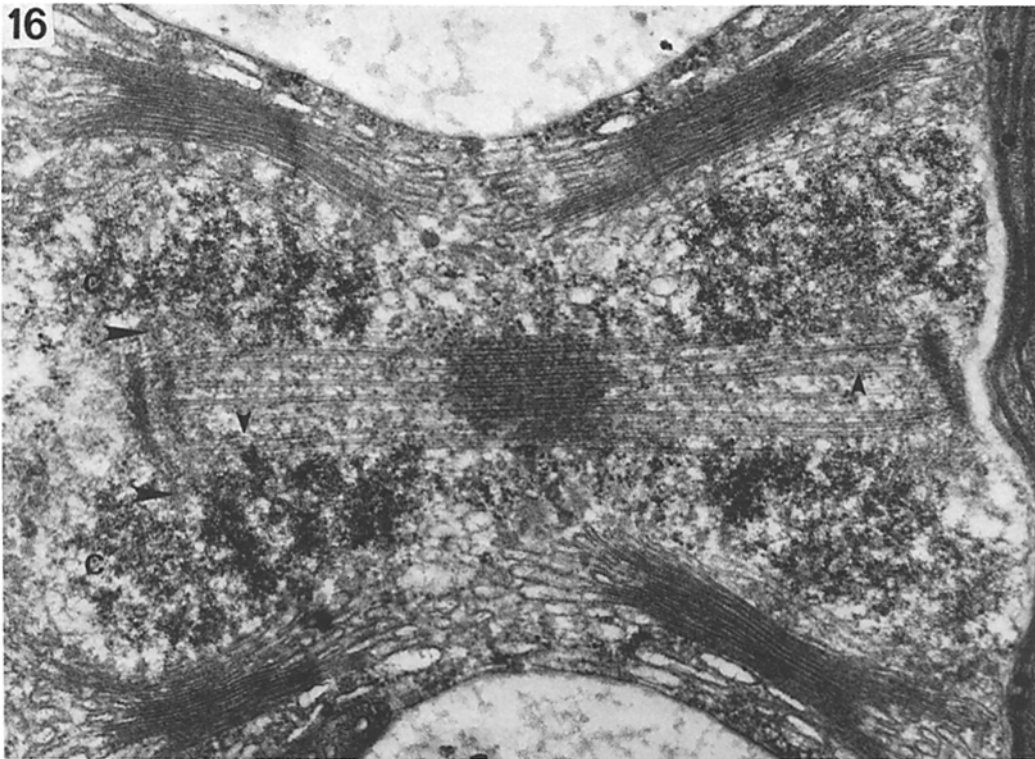


FIGURE 16 Late anaphase. The chromatin moves to the pole at early anaphase; then some of the chromatin (c) moves behind the polar complexes. The MTs of the central spindle are bowed outwards (small arrows) near the poles. The collar is evident near the poles (large arrows). $\times 38,000$.

FIGURE 17 Late anaphase sectioned at right angle to the cell in Fig. 16. Numerous MTs radiate laterally into the chromatin. In this view, some of the chromatin is behind the polar complex, but other chromatin (c) may be prevented from moving thus, possibly because it is blocked by the chloroplast. The cleavage furrow (arrow) will soon bisect the cell. $\times 38,000$.

because precise structural data from these spindles can be obtained. *Fragilaria* offers a small spindle that can be characterized with precision without backbreaking effort. For this paper nearly 80 spindles were analyzed in longitudinal sections (many more were not included because of technical problems such as both poles not present in one section), and 28 spindles were reconstructed from transverse serial sections. The arrangement of the cells into ribbons permits direct comparison of different mitotic stages from cells that are clones and nearly identical in size. Such comparisons allow confidence that the changes in the distribution of spindle MTs during mitosis do not merely result from cellular variation. We believe that this is the first time such information has been available from any mitotic system. Mitosis in *Fragilaria* appears representative of other diatoms thus far examined, although numerous minor differences in cell division are apparent between the different diatoms examined (18). The collar, recently discovered in *Surirella* (24) and most conspicuous in *Pinnularia* (19, 20), is clearly evident in *Fragilaria*, although we still cannot specify its functional or structural significance. The bowing out of MTs of the central spindle at the poles (Fig. 16) is similar to that observed in *Diatoma* (reference 17, Fig. 21) and *Pinnularia* (19, 20), and it may be caused by compressional forces generated during chromosomal movement to the poles. Movement of chromatin past the poles at telophase (see discussion in reference 24) and movement of the reformed MC to the completed cleavage furrow after cytokinesis is characteristic also of other diatoms. We feel that the results of this paper can be applied with some confidence to other diatoms, although minor anomalies between *Fragilaria* and other diatom spindles do exist.

General Comments on Tracking Spindle MTs

Certain technical problems make tracking MTs inherently subject to error. Even in the central spindle of this diatom, whose MTs are parallel and easy to track, the end points of some MTs are uncertain. Often, perhaps due to compression of the block face during sectioning, MTs do not line up in perfect register from one section to the next. Thus, human judgment is needed in assessing the optimum correlation of the MTs through sections. Other factors which also contribute to tracking errors include: (a) Occasionally one MT will start

sufficiently near the end point of another so that tracking these two MTs mistakenly indicates a single, continuous MT; (b) Obliquely sectioned MTs are especially difficult to track. Even using a goniometer stage when photographing the predominantly parallel MTs of the central spindle, it is occasionally not possible to tilt the section such that each MT projects a circular profile; (c) Because MTs generally do not lie straight between their end points, there are real positional changes between MT profiles along the length of the spindle.

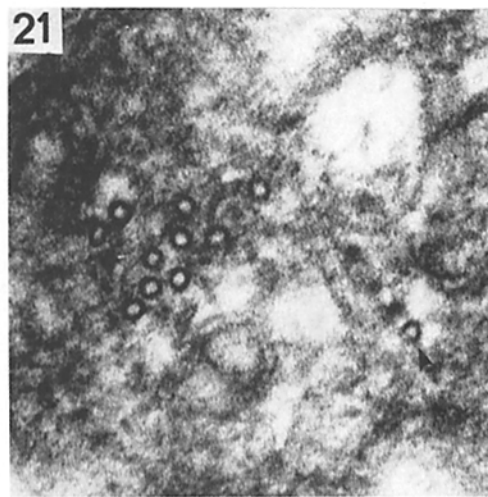
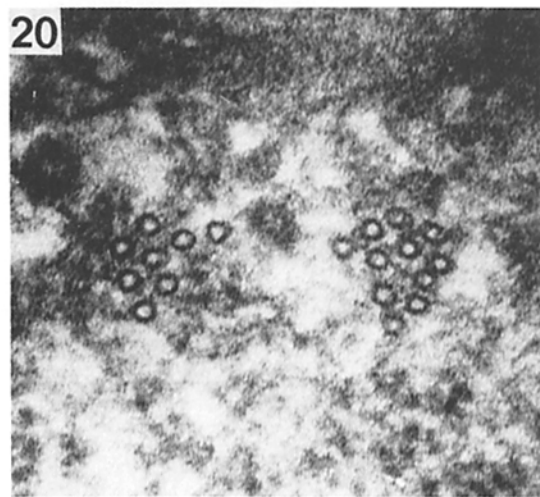
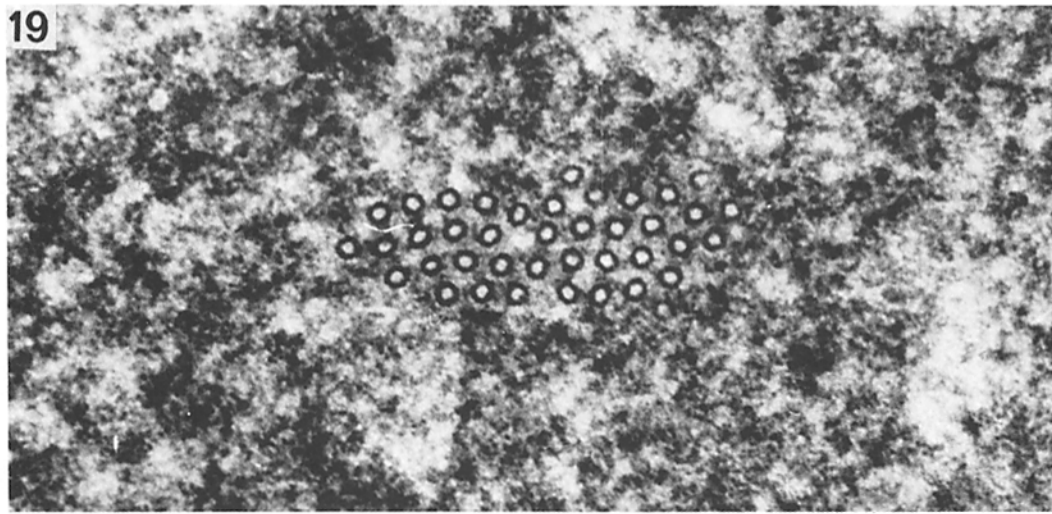
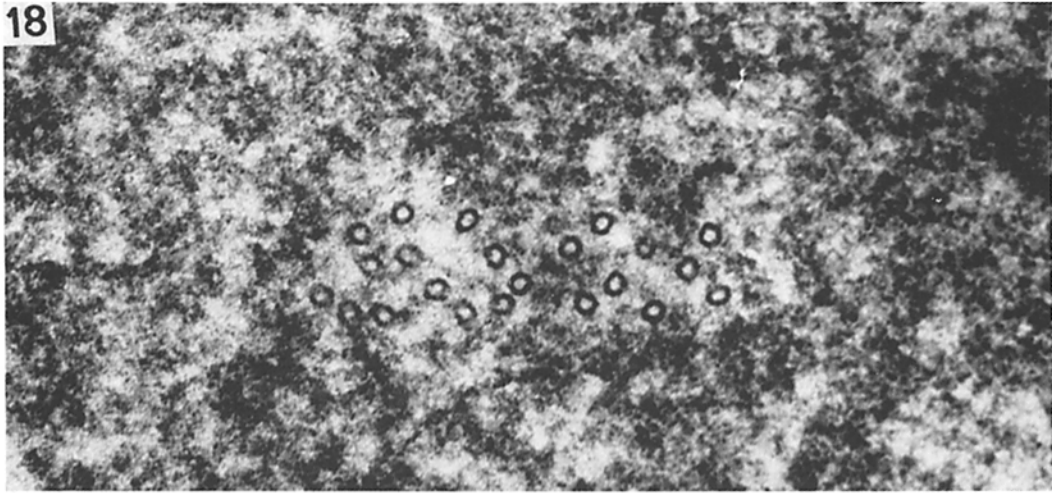
Despite these difficulties, we are absolutely confident of the assigned end point of each MT in at least 75% of the central spindles of *Fragilaria* that we have tracked.

Clearly, some cells have spindles more amenable than others for tracking MTs. For example, in the fungus *Uromyces*, a selected section through a metaphase half-spindle contains 108 MTs (7); in another fungus, *Thraustotheca*, this number is 41 (6); in yeast it is 21 (16), and in *Fragilaria* it is 21. In contrast, sections through the metaphase half-spindle of cultured human cells (HeLa) may contain ~2,400 ($\pm 20\%$) MTs (14), and those of higher plant cells (e.g., *Haemanthus*), ~1,700 MTs (8). Besides the enormity of the task of tracking MTs in these latter spindles, we believe that as the density of MTs within a spindle increases, so does the likelihood of tracking errors. For example, tracking over 1,000 MTs that converge towards the pericentriolar material is a formidable task not encountered in those smaller spindles that contain broad poles.

Funding priorities notwithstanding, we feel that the smaller spindles of the fungi, algae, and certain protozoa are more suitable using present techniques for MT tracking analysis than mammalian or higher-plant spindles.

The Prophase Spindle

The prophase central spindle consists predominantly of continuous MTs which increase in length as prophase progresses (Fig. 38A₁ and A₂). In contrast, the metaphase central spindle consists of two interdigitated half-spindles comprised mainly of polar MTs which overlap ~one-third of their length. The important question thus arises: does the prophase spindle consist of two interdigitated half-spindles which overlap their entire length? This, of course, would not be detectable from morphological observations since all the MTs sim-



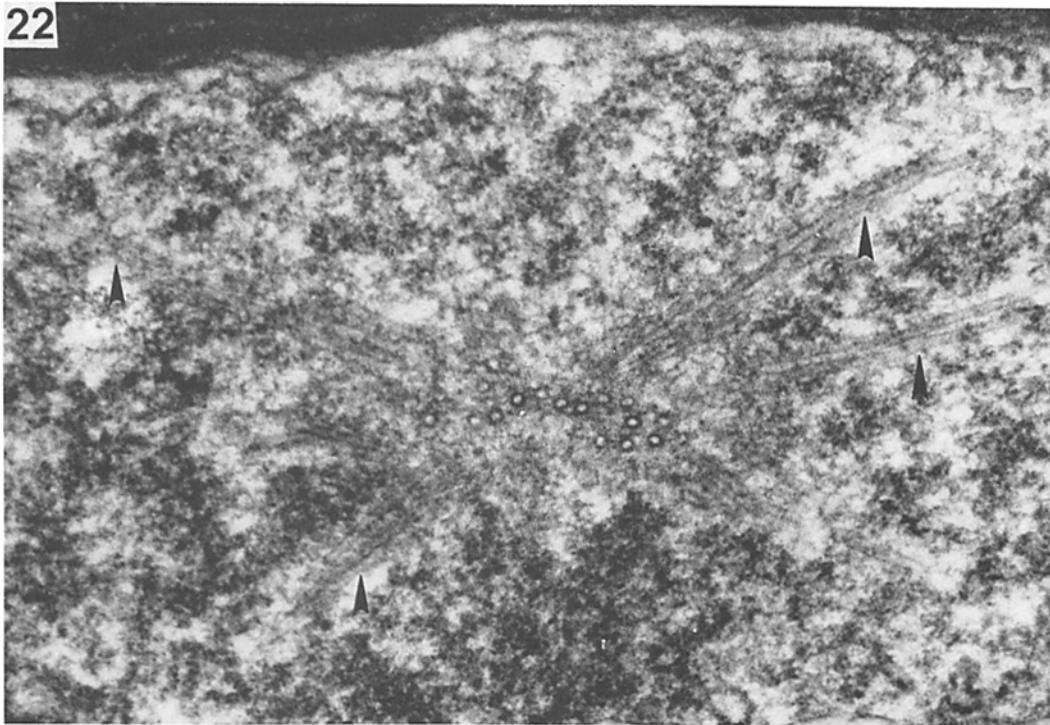


FIGURE 22 A micrograph of a section taken near the pole from the anaphase spindle similar to Fig. 16. Numerous MTs (arrows) radiate laterally from the pole and are nearly perpendicular to the central spindle. In a similar cell, these lateral MTs have been tracked through consecutive serial sections (see Fig. 34). $\times 70,000$.

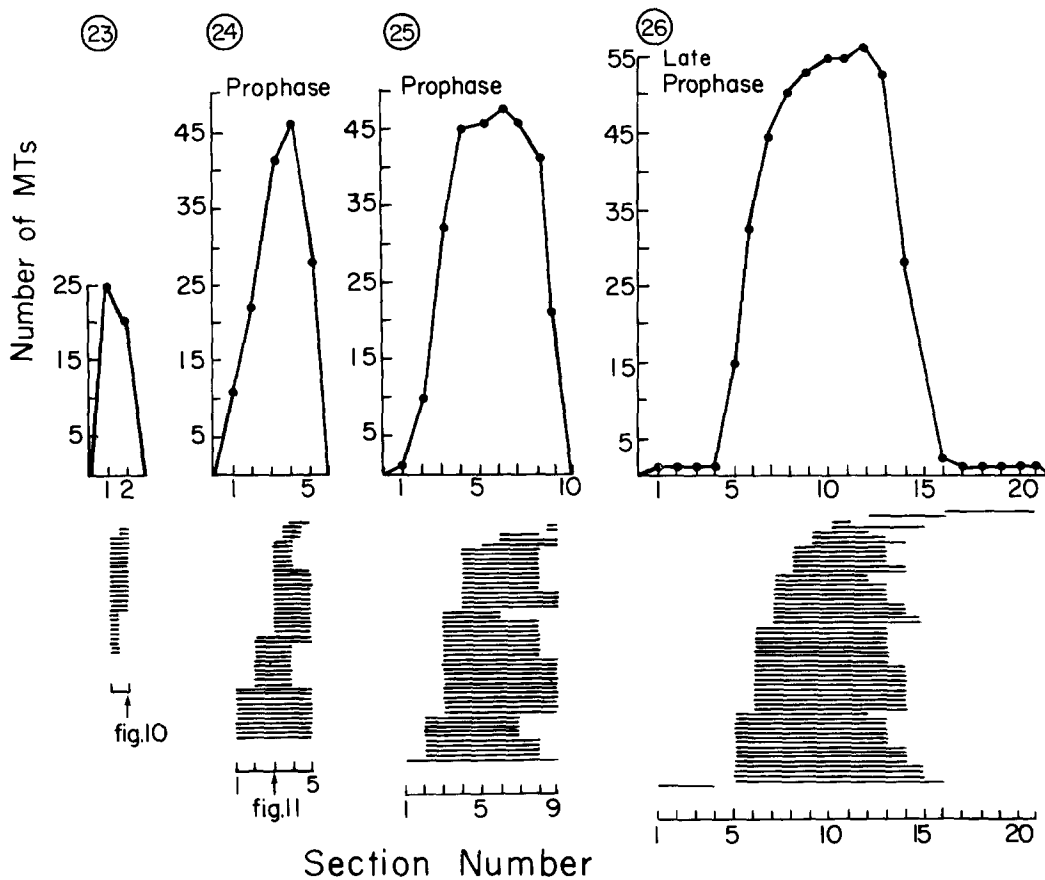
ply run from pole to pole. Also of interest is how the prophase spindle increases in length by addition of MT subunits. This problem has been briefly discussed (24), but without accompanying diagrams it is difficult to conceptualize the subtleties involved.

Several *in vitro* studies of MT polymerization indicate that MTs have an intrinsic polarity and a favored end of assembly and disassembly (10). If such properties are characteristic of the spindle MTs in diatoms, we can envisage different types

of diatom prophase spindles. First, assume that MTs nucleate (grow either at the distal or the proximal end) from one pole only. If all the MTs nucleating from the same pole are of the same polarity, then this spindle would contain MTs of one polarity (Fig. 38 B_1 —arrows assign an arbitrary polarity). Such a spindle could elongate by adding subunits preferentially to either end (Fig. 38 B_2), or at an equal rate at both ends. Second, MTs could nucleate from both poles and again if MTs of only one polarity nucleate from one pole,

FIGURES 18 and 19 Two micrographs through the metaphase spindle reconstructed in Fig. 29. The chromatin encircles the overlap region of the central spindle. The MTs in the overlap (Fig. 19) show evidence of both square and hexagonal packing. Near the pole (Fig. 18), the MTs of each half-spindle are arranged so that there are numerous spaces between them which correspond to the position of the MTs from the opposite pole in the overlap. $\times 106,500$.

FIGURES 20 and 21 Two micrographs through the telophase spindle reconstructed in Fig. 32. In contrast with metaphase, only a few MTs are now still overlapping (Fig. 21). The MT marked by the arrow is not included in the reconstruction (Fig. 32) because it is not part of the central spindle. The MTs of each half-spindle are grouped into two distinct bundles (Fig. 20). $\times 108,000$.



FIGURES 23-32 The groups of longitudinal lines in these figures are reconstructions of the central spindle at different stages of mitosis; each line represents an individual MT; collectively those lines show the end points of all the MTs in the central spindle (see text for detailed description). The serial number of each section through a given spindle, beginning at one pole and extending to the other, is set out along the horizontal axis. Each MT is identified and tracked through these serial sections, generating the horizontal lines which are arranged according to their length along the vertical axis. These diagrams do not show the spatial arrangement of MTs in the central spindle. For each prometaphase through telophase spindle, the reconstructions of its half spindles are displayed one on top of the other, i.e., all the MTs from one half-spindle are on the bottom of the diagram with those from the other above them. Above each reconstruction is the distribution of the total number of MTs in each section along the same spindle. The position of the chromatin during later stages of mitosis is indicated by the cross-hatching.

FIGURE 23 Early prophase spindle which is two sections long. Section 1 contains 25 MTs; 9 of these did not extend to section 2.

FIGURES 24 and 25 Early- and mid-prophase spindles which show successive stages in spindle development.

FIGURES 26 and 27 Late prophase spindles. The number and length of the MTs increases. Most of the MTs are continuous; variation in their length results from the polar complexes being tilted. For example in Fig. 26, parts of the polar complexes are contained in sections 5-8 and 12-14. Some MTs in Figs. 26 and 27 (the nine MTs at the top of the spindle in Fig. 27) extend past the pole away from the central spindle.

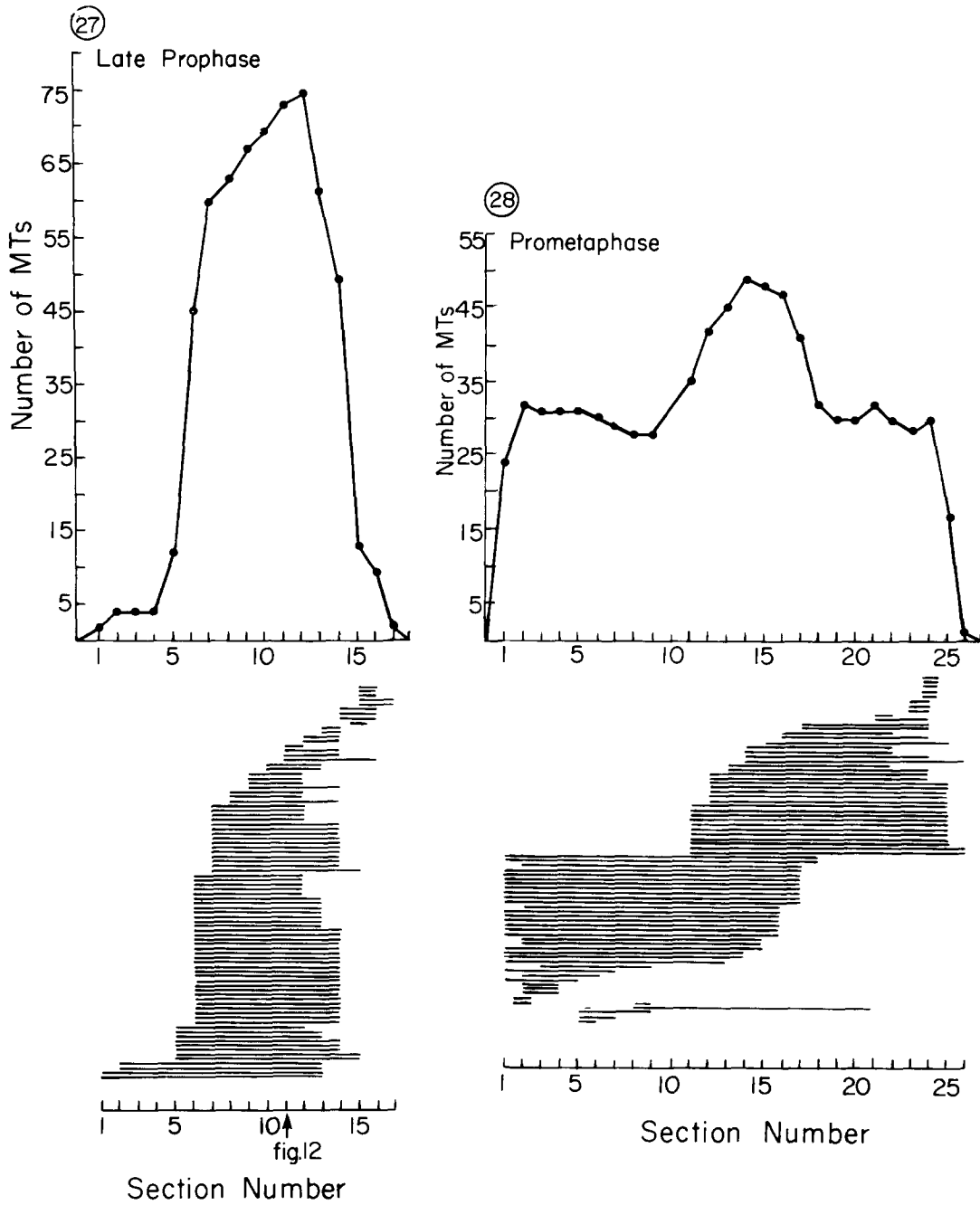


FIGURE 28 Prometaphase. The central spindle is composed of two interdigitated half-spindles containing no continuous MTs. The peak in the distribution profile corresponds to the overlap. The short MTs in sections 1-4 and 21-26 are located around the periphery of the central spindle.

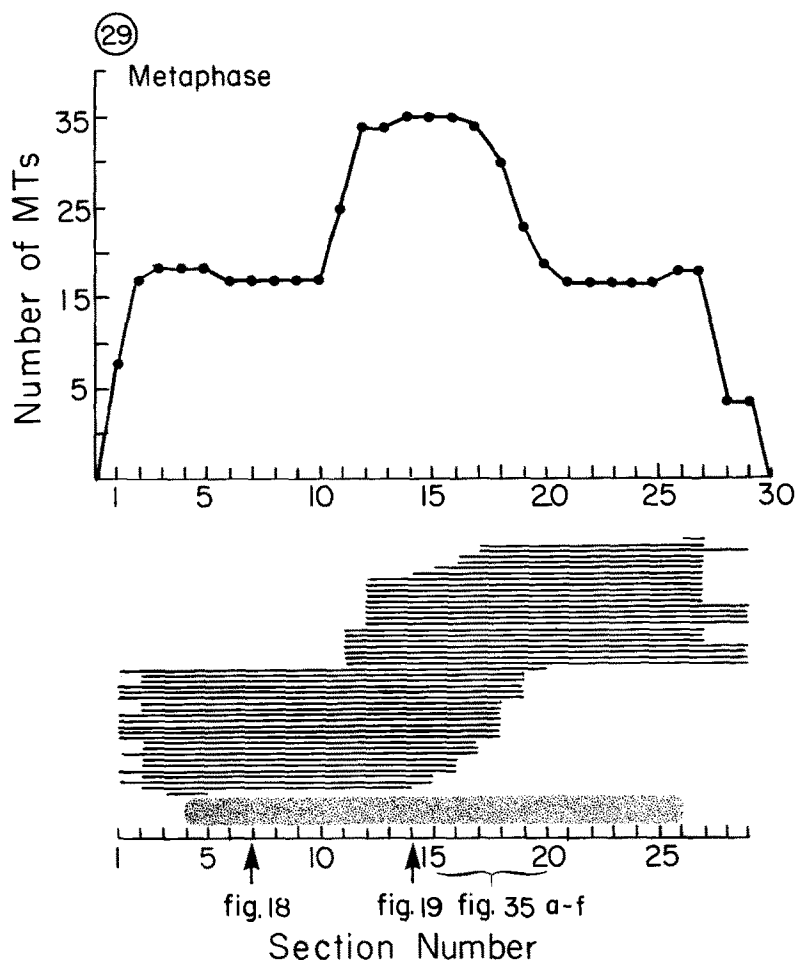


FIGURE 29 Metaphase. The chromatin encircles the central spindle which now contains fewer MTs than at late prophase and prometaphase.

this spindle would be composed of two sets of oppositely polarized MTs (Fig. 38C₁). To increase the spindle length, the MTs may add at an equal rate at both ends, or predominantly at either the distal or proximal end (proximal growth is shown in Fig. 38C₂). Such favored end growth would clearly necessitate a rearrangement (i.e., sliding) of MTs so as to keep all MTs running from pole to pole (24). Third, it is possible, but unlikely, that MTs of different polarities are nucleated from the same pole; in this case rearrangements of MTs (similar to Fig. 38C₂) would still be necessary to accommodate spindle growth.

We favor the second proposition, that the spindle is two sets of overlapping, oppositely polarized MTs (Fig. 38C₁). There is still no indication of

how the prophase spindle elongates. MT assembly alone could provide the force which separates the poles (i.e., equal growth at each end of the MTs); alternatively, sliding of MTs with concomitant polymerization could produce it.

Certain fungal spindles also appear to possess continuous MTs at prophase (11). Such continuous MTs are observed during later mitosis in other fungi where they appear to contribute to spindle elongation (3, 16, 22). Thus, the conceptual problem of understanding the elongation of the prophase spindle in *Fragilaria* is remarkably similar to that of elongation in anaphase spindles of fungi which contain continuous MTs. Perhaps, in certain fungi, growth of continuous MTs is responsible for elongating the spindle during all of mitosis,

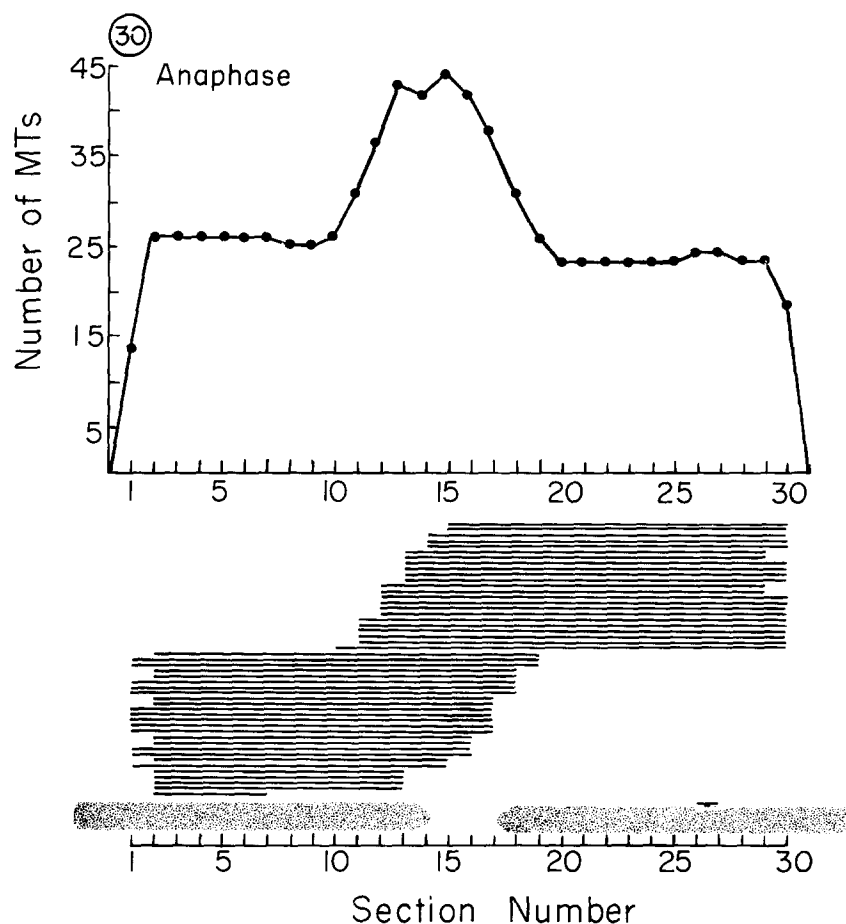


FIGURE 30 Anaphase. The chromatin has separated but the structure of the central spindle remains similar to metaphase.

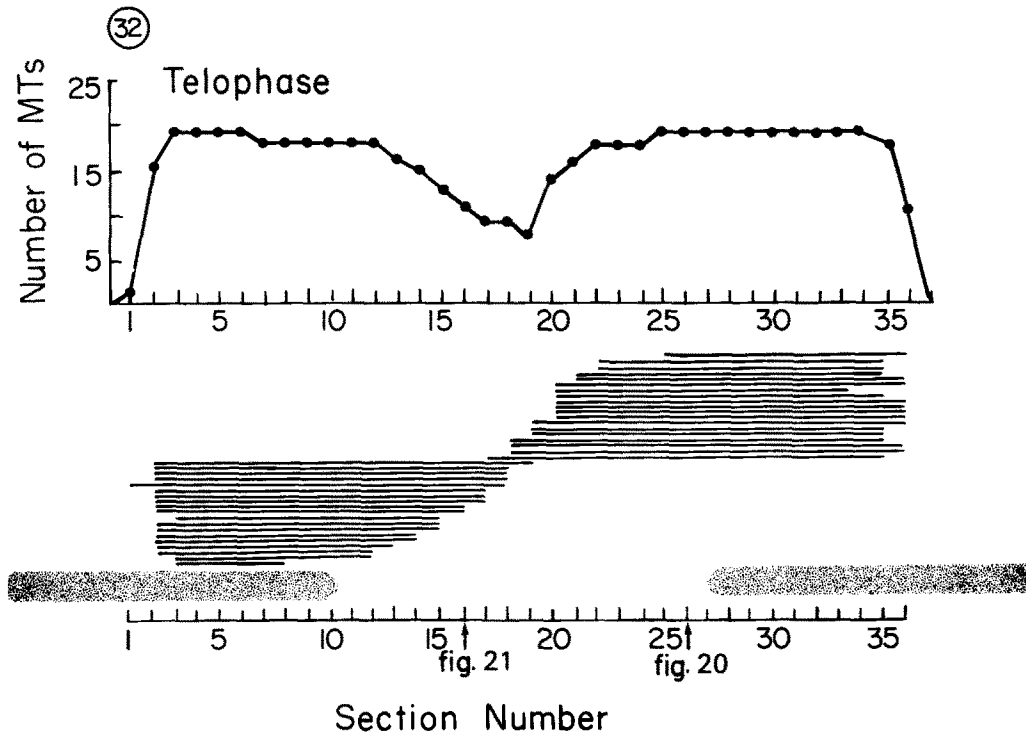
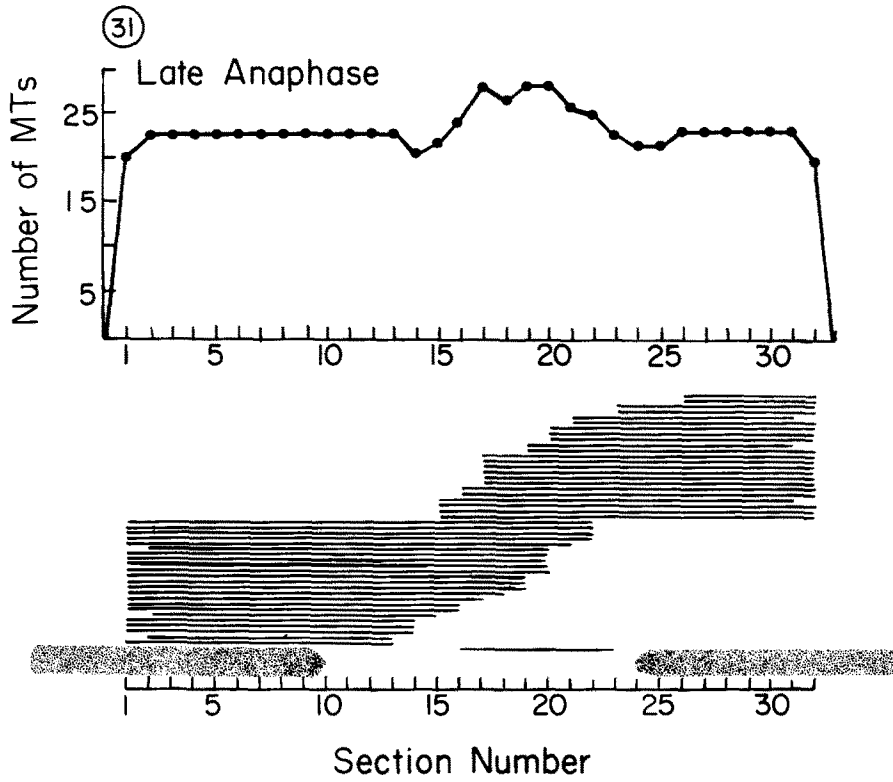
whereas in *Fragilaria* this process occurs only during prophase. The existence of such continuous MTs in higher plants and animals appears unlikely. However, this simple elongation described here may represent the most primitive type of spindle elongation, and may provide a useful system for the study of polymerization/depolymerization of MTs, and MT/MT interaction in production of force.

Rearrangement of MTs between Late Prophase and Prometaphase: Formation of the Two Half-Spindles

Between late prophase (Figs. 9a and 27) and prometaphase (Figs. 13 and 28), there are three major changes in the structure of the central spindle: (a) Its MTs at prophase are predominantly continuous, but by prometaphase it consists

of two interdigitated half-spindles comprised mainly of polar MTs and devoid of continuous MTs; (b) There is a rapid increase in the total spindle length; (c) The prophase (and prometaphase) spindle contains nearly 40% more MTs than the two half-spindles at metaphase and thereafter.

Our interpretation of these somewhat puzzling morphological changes is as follows: We suspect that the prophase spindle is two overlapping half-spindles which could then rapidly slide apart at late prophase, thereby reducing the overlap to the value observed at prometaphase while increasing the spindle length (Fig. 39). For example, the longest prophase spindle measured is 1.36 μm in length. If two sets of MTs in a spindle of this length slide apart but retain the portion of overlap observed at prometaphase (0.69 μm in the earliest prometaphase observed), then the corresponding



FIGURES 31 and 32 Late anaphase and telophase. The peak in the distribution profile declines (Fig. 31) and by late telophase (Fig. 32) there is a dip in the distribution curve; thus only a few MTs remain interdigitated in the overlap.

increased spindle length would be 2.03 μm . The measured spindle length of this prometaphase spindle is 2.62 μm . However, another prophase spindle (not included since both poles were not in the same section) had a length estimated at 1.47 μm , which is closer to the length of prometaphase half-spindles. Thus, if this prophase spindle slides as we have suggested above, each half-spindle may continue to elongate slightly after sliding

(i.e., by MT polymerization). Alternatively, the half-spindles may attain their full length before sliding, a stage we did not encounter and may have missed.

TABLE I
Number of MTs in the Central Spindle at Different Mitotic Stages

Stages of mitosis	Number of spindles analyzed	Number of MTs in the central spindle
Early prophase*	5	10, 16, 27, 28, 33
Mid-prophase	4	41, 43, 44, 45
Late prophase	3	57, 61, 86
Prometaphase	1	77
Metaphase	6	46, 47, 47, 47, 48, 50
Anaphase	8	41, 43, 45, 46, 46, 48, 48, 50
Telophase	3	38, 46, 46

* Stages of prophase are defined by spindle length (see Results, section entitled, Total Number . . .).

TABLE II
Frequency of Different Types of MTs in the Central Spindle

Stage of mitosis	Number of spindles analyzed	Continuous MTs	Polar MTs	Free MTs
Prophase	12	91*		
Prometaphase	1	0	92	8§
Metaphase	6	0	99.5	0.5
Anaphase	7	0.06‡	99.6	0.34
Telophase	2	0	96	4

* 91% of the prophase MTs are confirmed as continuous; the remaining 9% could not be positively identified for technical reasons (see Results, section entitled, Frequency of . . .).

‡ One continuous MT was identified in one spindle (see Discussion, section entitled, Continuous and Free MTs).

§ This prometaphase cell is shown in Fig. 28; the five MTs ending in section 22 are counted as free MTs.

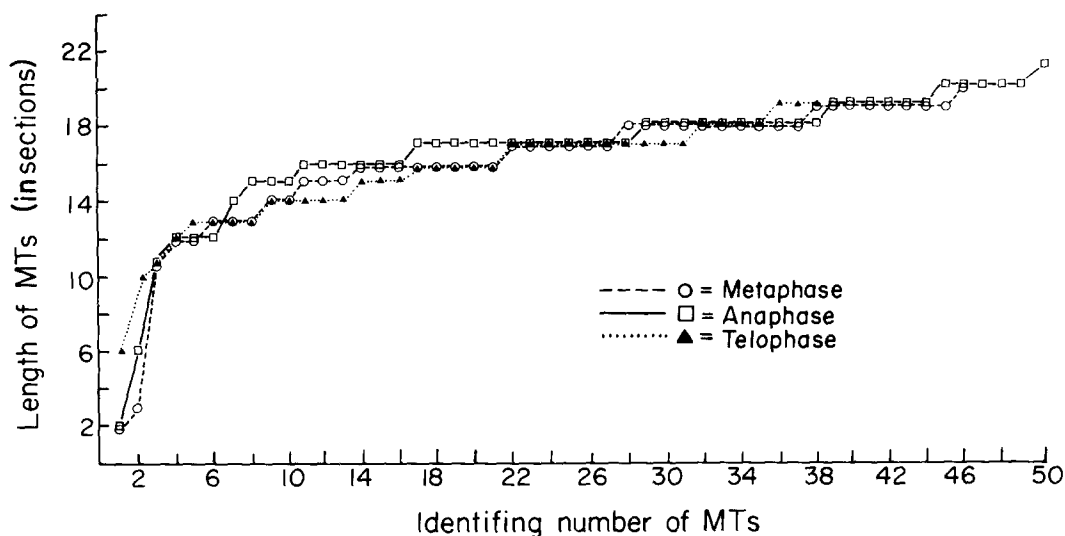


FIGURE 33 This graph shows the length of each MT of the central spindle of a metaphase, anaphase, and telophase spindle. The data for these three curves came from the spindles shown in Figs. 29, 30, and 32. Each curve is generated as follows: each MT from the spindle is arranged along the abscissa starting with the shortest and proceeding to the longest. The length of each MT (as determined by the number of sections it transverses) is plotted on the ordinate. For example, the metaphase spindle contains 46 MTs; MT no. 1 is two sections long, while MT no. 2 is three sections long, MT no. 3 is 11 sections long, and MTs nos. 4 and 5 are 12 sections long. The curves correspond closely indicating that the individual MTs in these spindles did not undergo changes in length during spindle elongation.

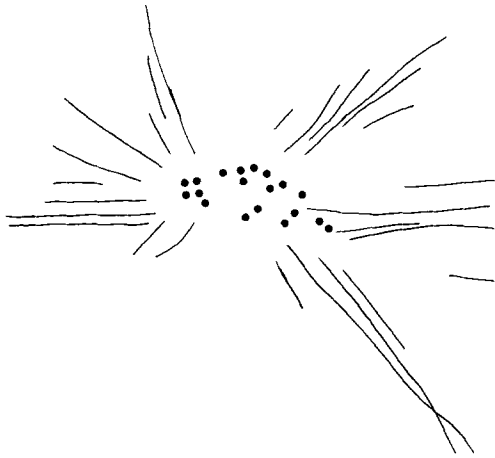


FIGURE 34 This drawing is a reconstruction (from six serial sections) of the MTs which radiate laterally from the spindle pole at late anaphase (see Fig. 22). Filled circles show the position of the central spindle MTs.

More complex explanations involving polymerization and depolymerization of MTs may also account for the changes in the spindle at late prophase, but appear less likely. Again, we assume that the prophase spindle is two overlapping half-spindles. At late prophase, disassembly of MTs could reduce the length of the overlapping portion of the half-spindles to the value observed at prometaphase (from 1.36 to 0.69 μm). Then the spindle could resume MT assembly such that the two half-spindles would be formed; starting with prometaphase overlap length, half the MTs could grow towards one pole and the remaining MTs grow towards the other. However, we have not observed any stages (such as prometaphase overlap length with the half-spindles just beginning to form) which suggest that this occurs. Alternatively, at late prophase, disassembly of half of the MTs from each pole could reduce the length of the overlapping portion of the half-spindles (from 1.36 to 0.69 μm), while the remaining MTs could increase in length by assembly (from 1.36 to 2.62 μm). In this case, the rate of MT assembly must occur at roughly twice the rate of disassembly, which somehow must be stopped when the appropriate overlap is formed.

The reduction in the number of MTs in the central spindle after prophase could be explained by assuming that some (but not all) of the MTs which radiated laterally from each pole at metaphase were, in fact, initially part of the prophase central spindle. During late prophase and prometaphase, some of the peripheral central spindle

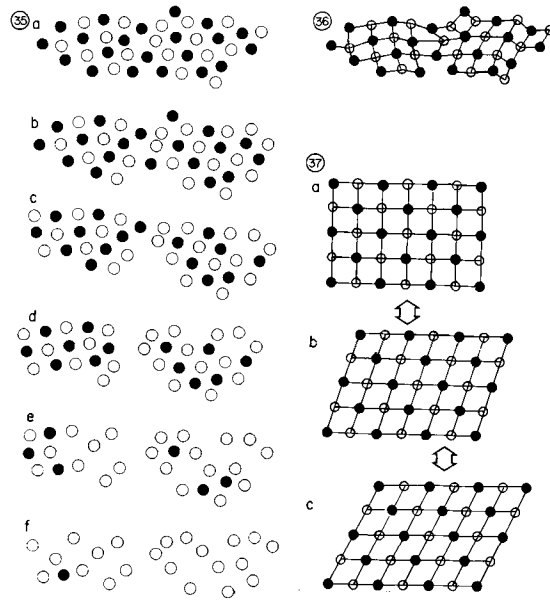


FIGURE 35 (a-f) These drawings are tracings of the MTs of the central spindle, taken from six consecutive serial sections in the metaphase spindle reconstructed in Fig. 29. The drawings show the spatial arrangement of MTs from opposite poles. Empty circles denote MTs from one pole while filled circles show those from the opposite pole. In the overlap (Fig. 35a) MTs are surrounded by those from the opposite pole. As the sections move progressively closer to the pole (Figs. 35b-f), MTs from one half-spindle drop out until those remaining are solely from the other half-spindle.

FIGURE 36 This diagram is generated by drawing lines through the rows of MTs from opposite poles in Fig. 35a. This procedure clarifies the irregularities in the packing of MTs in the overlap, while the MTs are neither perfectly square (Fig. 37a) or hexagonally (Fig. 37c) packed. Instead, a pattern of squares and rhomboids is generated.

FIGURE 37 (a-c) This diagram shows how square packing may be converted to hexagonal packing by displacing each row of MTs a certain distance sideways with respect to the next row (Figs. 37a, b and c; see Discussion). Filled circles denote MTs from one pole, and empty circles show those from the opposite pole. In square packing (Fig. 37a), each MT is surrounded by four MTs from the opposite pole; in hexagonal packing each MT is surrounded by two from the same pole and four from the opposite (Fig. 37c). Intermediate arrangements, which are neither perfectly square nor hexagonal, we call rhomboidal (Fig. 37b).

MTs could keep one end attached to the pole while they fan out radially, forming these lateral MTs. This assumption is strengthened by the fact

TABLE III
Length of the Overlap, Half Spindle, and Whole Spindle at Different Mitotic Stages*

Stage of mitosis	Cell no.	Whole spindle length	Average of the two half-spindle lengths	Overlap length
μm				
Metaphase	1‡	2.52	1.63	0.76
	2	2.48	1.62	0.72
	3§	2.62	1.68	0.76
	4	2.66	1.72	0.75
	5§	2.62	1.64	0.69
	6	2.61	1.64	0.67
	7	2.50	1.54	0.67
	8§	2.41	1.50	0.57
	9	2.64	1.63	0.64
	10	2.55	1.56	0.61
	11	2.52	1.54	0.59
	12	2.64	1.61	0.61
	13	2.76	1.68	0.59
	14	2.53	1.50	0.55
Anaphase	1	2.64	1.58	0.56
	2	2.75	1.64	0.56
	3	2.70	1.59	0.47
	4	2.73	1.60	0.47
	5	2.80	1.61	0.44
	6	2.83	1.63	0.42
	7	2.83	1.63	0.42
	8	2.80	1.61	0.42
	9	2.75	1.58	0.39
Telophase	1	2.83	1.58	0.36
	2	2.72	1.52	0.31
	3	2.75	1.53	0.31
	4	2.75	1.50	0.28
	5	2.76	1.52	0.28

* See text for discussion of accuracy of these measurements.

‡ The cells are arranged in this manner: The percent of the spindle length occupied by overlap is calculated. The spindle with the highest percent of overlap is listed first (cell 1) and the rest in descending order.

§ Prometaphase spindle.

that there are ~29 MTs radiating laterally from each pole (Fig. 34), which appear as the number of MTs of the central spindle decreases by ~40, or 20 per pole (i.e., 86 MTs in the late prophase spindle vs. ~47 at metaphase). Other explanations are possible; for example, a number of MTs in the central spindle could depolymerize and concurrently another set could assemble at the poles. If MTs do "peel off" the central spindle during prometaphase, this might be observable. As the spindle begins sinking into the nucleus,

certain MTs which are sufficiently close to the central spindle to have been part of it earlier invaginate the nuclear envelope; these may have peeled off the central spindle (Fig. 6).

Once the two half-spindles are formed at prometaphase, they do not appear to change significantly in length. In other larger diatoms, based upon observations from a limited number of cells, the half-spindles appear to increase in length during the later stages of mitosis, possibly contributing to spindle elongation (12, 17, 24). However, only observations on living cells may conclusively determine if the half-spindles in these larger diatoms increase in length.

Continuous and Free MTs

The existence of the small percentage of MTs that run from pole to pole in the central spindle

TABLE IV
Length of Overlap, Half-Spindle and Whole Spindle at Different Mitotic Stages Derived from a Ribbon of Cells (Clones)

Ribbon no.	Stage of mitosis	Whole spindle	Average of the two half-spindles	Overlap
μm				
1	Metaphase	2.48	1.62	0.72
	Metaphase	2.64	1.63	0.64
	Anaphase	2.83	1.63	0.42
	Telophase	2.83	1.58	0.36
2	Metaphase	2.52	1.54	0.59
	Anaphase	2.70	1.59	0.47
	Telophase	2.76	1.52	0.28

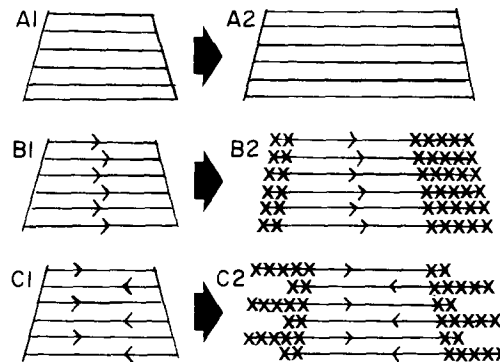


FIGURE 38 This figure illustrates how the prophase spindle may increase in length. A_1 shows a typical spindle at early prophase (e.g., Fig. 8) and A_2 at late prophase (Fig. 9a). The manner the spindle increases in length by addition of MT subunits (X) is shown in B_1 , B_2 , C_1 , C_2 ; see discussion for a detailed explanation.

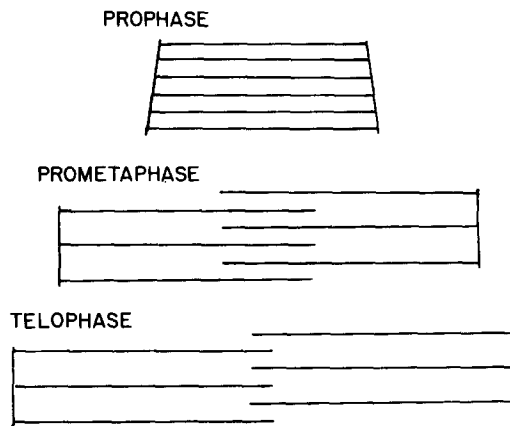


FIGURE 39 This diagram shows the structural changes which occur in the central spindle between prophase and telophase. Each line represents a single MT; for simplicity each spindle has only six MTs. These spindles are drawn roughly to scale representing the latest prophase, the earliest prometaphase and latest telophase spindles observed.

at metaphase is suggested by Manton et al. (9), on the basis of MT counts derived from transverse sections of the spindle of the centric diatom *Lithodesmium*. Tracking of MTs in transverse sections of the spindle of *Diatoma* (12) again indicates the existence of a few continuous MTs during metaphase and anaphase but none at telophase. These puzzling results raise the possibility that the continuous MTs are an important subpopulation whose function and reason for disappearance at telophase are obscure. One could conclude that in *Diatoma*, these continuous MTs elongate during anaphase (so that they still run from pole to pole) but then break by telophase. In *Fragilaria*, spindle MTs can be more accurately tracked than in *Diatoma* since the spindle is shorter and contains fewer MTs. In *Fragilaria*, there are no continuous MTs between prometaphase and telophase in 15 spindles, and one in a single metaphase spindle. This latter exception we believe to be the result of tracking error. Similarly, in *Diatoma* the continuous MTs may also be illusory, resulting in tracking errors (a fortuitous juxtaposition of the end of one polar MT with the beginning of another from the opposite half-spindle, such that these two MTs appear to register over one or two sections; the resulting track would indicate the existence of a continuous MT). Because continuous MTs are not consistently observed in *Fragilaria* after prophase, we conclude that they do not consti-

tute a significant component of this central spindle, nor are they necessary for spindle function during later mitosis. Likewise, free MTs are present in the central spindle of both *Diatoma* and *Fragilaria*. Some of these, but definitely not all, could be ascribed to tracking errors. Because nine of these 16 spindles that we tracked (after metaphase) contained no free MTs, we conclude that they also are not a functional component of the central spindle of *Fragilaria*. The possibility that certain MTs are lost during preparation cannot be excluded.

Rearrangement of MTs at Anaphase-Telophase

At late anaphase, the length of overlap decreases and the spindle length increases; the easiest way to explain these changes in *Diatoma* (12) and *Fragilaria* is to postulate that the MTs of the half-spindles slide past one another (Fig. 39). If such sliding occurs, the decrease in length of the overlap should equal the increase in spindle length, if the half-spindles are the same length. In *Fragilaria*, the lengths of the overlap and the half-spindles were measured. However, these measurements are not precise for the following reasons: (a) The overlap as measured from longitudinal sections is not precisely defined since the MTs of each half-spindle vary in length and thus do not end at the same point in the overlap: only a subjective measurement of the overlap is possible; (b) From transverse serial sections, the average overlap can be determined more precisely from reconstructed spindles, but variation in section thickness may create inaccuracies when determining its length in microns.

Therefore, a comparison of the decrease in overlap length with the increase in spindle length must be made with caution. From reconstructed spindles derived from the same ribbon (clones), the spindle increases in length about seven sections between metaphase and telophase while the decrease in the maximum extent of overlap is also about seven sections (see Results). In longitudinal sections of spindles from two ribbons of cells, the decrease in overlap from metaphase to telophase is $0.36 \mu\text{m}$ in one, and $0.31 \mu\text{m}$ in the other ribbon, while the spindle length increases by 0.35 and $0.24 \mu\text{m}$ respectively. There are discrepancies in the data when comparing the longitudinally sectioned spindles with the transversely sectioned spindles. For example, if we assume a section thickness of 80 nm , then the spindle length at

metaphase is calculated to be $2.16 \mu\text{m}$ (see section entitled, Indirect Length . . .), $0.32 \mu\text{m}$ shorter than the measured values from longitudinal sections in ribbon 1, Table IV. Similarly, the telophase spindle is $0.11 \mu\text{m}$ shorter. Part of this difference could result from variation in section thickness. The decrease in overlap (seven sections at 80 nm per section) would be equivalent to $0.56 \mu\text{m}$; in longitudinal sections, the largest decrease (within the same ribbon of cells) was only $0.36 \mu\text{m}$. We wish to emphasize that there are various intermediates of metaphase and telophase, and thus a comparison of one longitudinally sectioned telophase with another reconstructed telophase may be inaccurate. For example, the maximum extent of overlap in the telophase spindle (Fig. 32) is three sections or $0.24 \mu\text{m}$ (80 nm per section). Thus if the telophase spindle in Table IV (ribbon 1) reduced its overlap to $0.24 \mu\text{m}$, then the decrease in overlap from metaphase to telophase would equal $0.48 \mu\text{m}$, which is close to the value calculated from transverse sections.

Therefore, the data on length of the overlap and whole spindle suggest, but do not definitely determine, whether the half-spindles slide apart, or whether at metaphase, anaphase, and telophase the MTs of each half-spindle depolymerize at their free ends (overlap) concurrently with polymerization at the poles. The sliding proposition is supported by the observation that the lengths of individual MTs that constitute the half-spindle are about the same at metaphase, anaphase, and telophase in a single ribbon of cells (Fig. 33). At metaphase, the shortest and longest MTs appear randomly intermingled in the overlap. By telophase and the maximum extent of spindle elongation, only the longest MTs in each half-spindle remain in the shortened overlap (Fig. 21). This observation suggests that MTs slide past one another as far as possible—to the limit of the overlap that can remain using the longest MTs. Furthermore, as the shorter MTs move out of the overlap, the longer ones appear to close in together (“zip”—reference 1).

The MTs in each half-spindle of *Fragilaria* closer to the pole also undergo an accompanying rearrangement at telophase, as they tend to clump (zip), often into two distinct groups. Similar rearrangement of MTs appears at telophase in the much larger spindle of *Pinnularia* (20), when numerous small clusters of MTs (5–20) arise in each half-spindle, which now often develops a pronounced twist. Thus, quite active structural changes (e.g., in the packing of MTs)

in each half-spindle probably accompany spindle elongation.

Interaction of MTs in the Overlap

While various different patterns of MT packing are known (see reference 25), reports of close packing in spindle MTs are rare. Heat-shocked kinetochore MTs of *Haemanthus* form hexagonally packed MT bundles (21). Such systems generally contain MTs which are presumably of the same polarity (derived from one organizing center which nucleates MTs of all one polarity). In contrast, diatom spindles contain two close-packed interacting sets of MTs which are from opposite poles and presumably are of opposite polarity. Thus, the diatom spindle can display the packing arrangement given by MTs of the same (in the half-spindles) or different (in the overlap) polarities.

The prophase spindle of *Melosira* comprises a remarkably regular arrangement of square-packed MTs. This packing has further significance, because one MT from one pole is usually surrounded by four from the opposite pole (23). In the overlap of other diatoms, such as *Surirella* (24), and *Pinnularia* (19, 20), the MTs are not so regularly arrayed, but domains of square packing are clearly present. In *Fragilaria*, the square and hexagonal packing of MTs is not perfect, but tracking confirms that the interdigitation of MTs in the overlap, which are square packed, is equivalent to *Melosira*; in hexagonally packed domains, each MT is surrounded by six others, but again this arrangement has additional significance because each MT is surrounded by two from the same pole and four from the opposite. (Theoretically, it is not possible to surround the central MT alternately by three MTs from each pole and then to propagate such an arrangement indefinitely in two dimensions.)

The overlap of *Fragilaria* always displays irregularities in the pattern of MTs which do not precisely conform to either square or hexagonal packing. To help clarify the nature of these irregularities (as in Fig. 35a), we traced lines through rows of MTs from opposite poles. In square packing (as in *Melosira*), this procedure obviously gives rise to a square grid (Fig. 37a), but in the overlap of *Fragilaria* a pattern of squares and rhomboids is generated (Fig. 36, derived from Fig. 35a). Such a pattern shows varying degrees of translation between the rows of MTs so that they are neither in perfect square or hexagonal packing. All these intermediate

arrangements between square (Fig. 37a) and hexagonal (Fig. 37c) we call "rhomboidal" packing (Fig. 37b), and Fig. 37a-c shows how perfect square and hexagonal packing arrangements are thus interconvertible via rhomboidal intermediates. Such displacement may explain the irregularities in the packing of the overlap in diatoms. Rhomboidal packing is also characteristic of the MTs in the axostyle of the protozoan *Saccinobaculus* (15) where curvature of the axostyle causes its constituent rows of MTs to change their packing from hexagonal through rhomboidal to square. In conclusion, tracking the MTs in the spindle of *Fragilaria* has demonstrated what may be a fundamental characteristic of the diatom spindle generally; namely, the nature of the nonrandom interdigitation of two sets from opposite spindle poles and presumably of opposite polarity. Furthermore, if square packing is converted through rhomboidal to hexagonal packing (as in Fig. 37a-c), each MT from one pole in all cases can theoretically remain bridged to four from the opposite pole. Therefore, hexagonal, rhomboidal, and square packing may all be functionally equivalent, even though hexagonal packing may be thermodynamically more stable.

Mechanism of Spindle Elongation in Fragilaria: Conclusions

Elongation (separation of the poles) of the central spindle in *Fragilaria* proceeds in two stages. First, the early prophase spindle, which contains predominantly pole-to-pole MTs, elongates. During this stage, there is no observable redistribution of spindle MTs as the spindle elongates (they remain pole-to-pole). The two most likely means of achieving this elongation are: (a) polymerization of MTs and (b) polymerization concomitant with sliding of MTs. Second, at late prophase and late anaphase there are redistributions of MTs in the central spindle concurrent with spindle elongation; these changes are not involved in chromosomal movement to the poles, which occurs separately. The most likely means of achieving these latter two redistributions (late prophase and late anaphase) of spindle MTs are: (a) polymerization and depolymerization of MTs and (b) sliding of MTs, i.e., sliding apart of the half-spindles. We favor the sliding proposition, in part because the transition from late prophase to prometaphase would

be especially difficult to envisage as occurring by polymerization-depolymerization. If such sliding occurs, it may be passive, or it may be active sliding generated by mechanochemical mechanisms operative in the overlap. The latter could be accomplished by packing of MTs from opposite poles in the overlap sufficiently close to permit cross-bridging (and sliding) between MTs from opposite poles. What stops the presumed sliding at prometaphase and restarts it at anaphase is not known. However, arrest of prometaphase sliding could result from attachment of unseparated paired chromatids to opposite spindle poles (or collars), thereby limiting the extent of sliding and separation of the poles at this stage. Later, after the chromosomes separate at anaphase, the half-spindles could resume sliding apart.

Anaphase spindle elongation has generally been considered a process generated specifically to further separate the daughter chromosomes at anaphase. However, this may be a limited view of spindle elongation. The possibility that prophase and anaphase spindle elongation is a continuous process interrupted by chromosome attachment to the spindle may profitably be applied to other mitotic cells. The control mechanisms necessary in such a model of spindle elongation are reduced in complexity, perhaps being effected solely by chromosome splitting, which has previously been shown to occur independently of pole-directed forces.

In this and previous work on the diatom spindle, we have consistently favored the idea that MT sliding in part generates spindle elongation. Other, more complicated explanations which fit our data cannot be ruled out. Of course, morphological evidence alone cannot prove that sliding occurs *in vivo*.

The authors wish to thank J. R. McIntosh for useful discussions concerning MT polarity.

This work was supported by a grant from the National Science Foundation, grant PCM76-18287. Dr. Schulz was supported by a fellowship from the Max Kade Foundation, New York.

Received for publication 20 March 1978, and in revised form 14 August 1978.

REFERENCES

1. BAJER, A. 1973. Interaction of microtubules and the mechanism of chromosome movements (Zipper hypothesis). I. General principle. *Cytobios.* 8:249-281.

2. BRINKLEY, B. R., and J. CARTWRIGHT, JR. 1971. Ultrastructural analysis of mitotic spindle elongation in mammalian cells *in vitro*. *J. Cell Biol.* **50**:416-431.
3. FRANKE, W. W., and P. DEAN. 1973. The mitotic apparatus of a Zygomycete, *Phycomyces blakesleeana*. *Arch. Mikrobiol.* **90**:121-129.
4. FUGE, H. 1973. Verteilung der Mikrotubuli in Metaphase- und Anaphase-Spindeln der Spermatozyten von *Pales ferruginea*. *Chromosoma (Berl.)*. **43**:109-143.
5. FUGE, H. 1974. The arrangement of microtubules and the attachment of chromosomes to the spindle during anaphase in tipulid spermatozytes. *Chromosoma (Berl.)*. **45**:245-260.
6. HEATH, I. B. 1974. Mitosis in the fungus *Thraustotheca clavata*. *J. Cell Biol.* **60**:204-220.
7. HEATH, I. B., and M. C. HEATH. 1976. Ultrastructure of mitosis in the cowpea rust fungus *Uromyces phaseoli* var. *vignae*. *J. Cell Biol.* **70**:592-607.
8. JENSEN, C., and A. BAJER. 1973. Spindle dynamics and the arrangement of microtubules. *Chromosoma (Berl.)*. **44**:73-89.
9. MANTON, I., K. KOWALLIK, and H. A. VON STOSCH. 1970. Observations on the fine structure and development of the spindle at mitosis and meiosis in a marine centric diatom (*Lithodesmium undulatum*). III. The later stages of meiosis I in male gametogenesis. *J. Cell Sci.* **6**:131-157.
10. MARGOLIS, R. L. and L. WILSON. 1978. Opposite end assembly and disassembly of microtubules at steady state *in vitro*. *Cell*. **13**:1-18.
11. McCULLY, E. K., and C. F. ROBINOW. 1973. Mitosis in *Mucor Hiemalis*: A comparative light and electron microscopic study. *Arch. Mikrobiol.* **94**:133-148.
12. McDONALD, K. D., J. D. PICKETT-HEAPS, J. R. MCINTOSH, and D. H. TIPPIT. 1977. On the mechanism of anaphase elongation in *Diatoma vulgare*. *J. Cell Biol.* **74**:377-388.
13. MCINTOSH, J. R., W. Z. CANDE, and J. A. SNYDER. 1975. Structure and physiology of the mammalian mitotic spindle. In *Molecules and Cell Movement*. S. Inoue, and R. E. Stephens, editors. Raven Press, New York. 31-76.
14. MCINTOSH, J. R., and S. C. LANDIS. 1971. The distribution of spindle microtubules during mitosis in cultured human cells. *J. Cell Biol.* **49**:468-497.
15. MCINTOSH, J. R., E. S. OGATA, and S. C. LANDIS. 1973. The axostyle of *Saccinobaculus*. I. The structure of the organism and its microtubule bundle. *J. Cell Biol.* **56**:304-323.
16. PETERSON, J. B., and H. RIS. 1976. Electron microscopic study of the spindle and chromosome movement in the yeast *Saccharomyces cerevisiae*. *J. Cell Sci.* **22**:219-242.
17. PICKETT-HEAPS, J. D., K. L. McDONALD, and D. H. TIPPIT. 1975. Cell division in the pennate diatom *Diatoma vulgare*. *Protoplasma*. **86**:205-242.
18. PICKETT-HEAPS, J. D., and D. H. TIPPIT. 1978. The diatom spindle in perspective. *Cell*. **14**:455-467.
19. PICKETT-HEAPS, J. D., D. H. TIPPIT, and J. ANDREOZZI. 1978. Cell division in the pennate diatom *Pinnularia*. I. Early stages of mitosis. *J. Biol. Cellulare (Paris)*. **33**.
20. PICKETT-HEAPS, J. D., D. H. TIPPIT, and J. ANDREOZZI. 1978. Cell division in the pennate diatom *Pinnularia*. II. Later stages of mitosis. *J. Biol. Cellulare (Paris)*. **33**.
21. REIDER, C., and A. S. BAJER. 1977. Heat induced reversible hexagonal packing of spindle microtubules. *J. Cell Biol.* **74**:717-725.
22. ROOS, U. P. 1975. Mitosis in the cellular slime mold *Polysphondylium violaceum*. *J. Cell Biol.* **64**:480-491.
23. TIPPIT, D. H., K. L. McDONALD, and J. D. PICKETT-HEAPS. 1975. Cell division in the centric diatom *Melosira varians*. *Cytobiologie*. **12**:28-51.
24. TIPPIT, D. H., and J. D. PICKETT-HEAPS. 1977. Cell division in the pennate diatom *Surirella ovalis*. *J. Cell Biol.* **73**:702-727.
25. TUCKER, J. 1977. Shape and pattern specification during microtubule assembly. *Nature (Lond.)*. **266**:22-26.